A Role of Pore Air in Infiltration Process

AUTHOR(S):

ISHIHARA, Yasuo; SHIMOJINIA, Eiichi

CITATION:

ISHIHARA, Yasuo ...[et al]. A Role of Pore Air in Infiltration Process. Bulletin of the Disaster Prevention Research Institute 1983, 33(4): 163-222

ISSUE DATE:

1983-12

URL:

http://hdl.handle.net/2433/124921

Bull. Disast. Prev. Res. Inst., Kyoto Univ., Vol. 33, Part 4, No. 302, December, 1983

A Role of Pore Air in Infiltration Process

By Yasuo ISHIHARA and Eiichi SHIMOJIMA

(Manuscript received October 3, 1983)

Abstract

This paper deals with an investigation on the mechanism of confined infiltration under a ponding condition at the surface of the sand layer, especially the mechanism of exchange of the penetrating water and the air in such a layer.

After carrying out experiments of ponded infiltration with a constant water depth into a homogeneous and air-dried sand layer in a lucite cylinder with a bottom plate, a theoretical analysis is undertaken by considering such an infiltration as continuous and simultaneous flows of water and air in average by referring to results of a supplementary experiment of the exchange of liquid and air in a U-shaped tube. And then, the analytical results are compared with the experimental ones.

The results disclose the following: 1) The moisture profile is formed by quasi-saturated zone (QSZ) and unsaturated zone (USZ). The QSZ develops in the neighbourhood of the sand surface, and as time goes on, it declines in development and approaches a certain depth asymptotically. The USZ continues to develop accompaning by the downward movement of the wetting front. 2) Although, strictly speaking, the infiltration process is discontinuous because of an intermittent escape of pore-air from the sand surface, such a process can be dealt with, in average as continuous. The movement of water and air obeys the law of Darcy's type in the QSZ and the generalized Darcy's law in the USZ. 3) The QSZ which is developing through a formation stage has a significant effect on the air escape. Its resistance becomes at least several times as large as one in the USZ. The escape condition is determined at the lower end of the QSZ by the thickness of such a zone, the water entry value and the ponding depth. 4) In stage where the QSZ is being formed and has developed enough, characteristic behaviour of water and air appear.

1. Introduction

It is well known that the infiltration phenomenon of rain-water into the ground plays a very important role in hydrologic cycle and, practically, in the problem of water resources. A large fraction of falling water as rain on a land surface penetrates through unsaturated soil strata, which is known as the process of infiltration. As a rock surface or ground water surface usually exists beneath the ground, the field of infiltration is the finite domain between the land surface and the lower boundary mentioned above. As the air in the voids of the domain cannot move through the lower boundary, the air to be displaced by penetrating water escapes only through the surface of the land into the atmosphere. However, when the water content in the neighbourhood of a land surface becomes large or when ponding occurs on a land surface, the air is considered to be unable to escape into the atmosphere freely. As a result, the dynamics of the process of infiltration becomes very complicated.

If we examine the studies on such an infiltration historically, it was done roughly in three stages. The first is a germinal stage from 1935 to 1940, and only experi-

mental studies were done by Power[1], Horton[2], Free and Palmer[3], et al.. These were limited to the description of phenomena. The second stage occurs in the 1960's. These are the full-dress studies on infiltration mechanism with experiments. However, the majority are too microscopic to understand the infiltration process in totality. These were done by Wilson and Luthin[4], Youngs and Peck[5], Peck[6,7], Ishihara, Takagi and Baba[8], Takagi and Baba[9], et al.. The final stage occurs in the 1970's. These largely consisted of theoretical or analytical studies by numerical calculation. The behaviour of pore-air is dealt with dynamically and infiltration is recognized as being simultaneous flows of water and air. These investigations were done by Brustkern and Morel-Seytoux[10,11], McWhorter[12], Noblanc and Morel-Seytoux[13], Sono and Morel-Seytoux[14], et al.. However, in spite of these excellent studies, the following problems still remain. In order to understand the process of infiltration under a ponding condition at the land surface, that is so-called ponded infiltration, how do we introduce the phenomenon of repeated and intermittent air escape into fundamental equations of water and air? And more essentially, what is the exchange mechanism of both phases?

In order to clarify such an infiltration process, especially by paying attention to the effect of pore-air on penetrating water, the experiments of ponded infiltration, firstly, are carried out by a homogeneous and initially air-dried sand-layer with a lower solid boundary. Next, the results obtained are discussed in light of the facts which are obtained by a supplementary experiment on the exchange of liquid and air, using a U-shaped capillary tube. Finally, a theoretical analysis is undertaken by considering such an infiltration process as the continuous and simultaneous flow of water and air by averaging in certain scales of time and space, and the analytical results are compared with the experimental ones.

2. Result of the experiment[15]

2.1 Apparatus and method of the experiment

A vertical and homogeneous infiltration field is made by two kinds of naturally air-dried sand, Sand K-7 and Sand K-6 in **Fig. 1**, being inserted into a lucite cylinder of 18.5 cm in inner diameter with a bottom plate. The cylinder is built up by combining segments of cylinders of 25 cm, 20 cm and 10 cm in length with flanges at both ends. The top segment of the constructed cylinder has a receiver for water overflowing from its upper part. So, the length of the cylinder is changeable. The upper boundary of sand column, *i.e.*, the sand surface is horizontal and is under the upper edge of cylinder to make a pond on the sand surface. The degree of compactness of sand column is $1.41 \sim 1.39\ \mathrm{gr/cm^3}$ for Sand K-7 and $1.43 \sim 1.42\ \mathrm{gr/cm^3}$ for Sand K-6, and the porosity is almost 0.46 in both.

Water is supplied on the sand surface at such a constant rate that some water is always overflowing from the upper edge of the cylinder. Especially, at the beginning of experiment, a large quantity of water is supplied to the sand surface so that

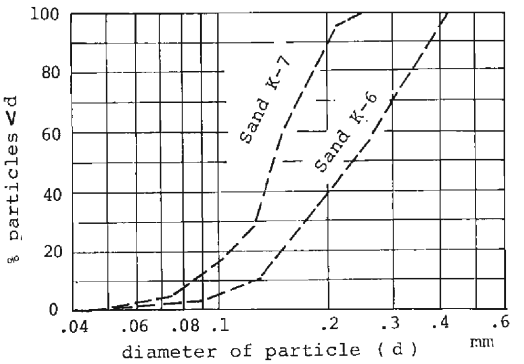

Fig. 1. Particle-size distribution.

a pond of decided depth is instantly formed. The ponding depth is always held constant.

The infiltration rate, moisture content and pore-air pressure are measured. The infiltration rate is estimated by subtracting the discharge of overflowing water mentioned above, being measured by a weir with a pressure gauge, from the rate of water supply. Moisture content is measured by an electric capacitance method where a pair of metal plates with 1 cm in width and 18 cm in length are placed on the outer side of cylinder in a circumfluent direction, being symmetric with respect to the axis of the cylinder. The measurement points are 10~15 cm apart from each other in depth. Pore-air pressure is measured by a pressure gauge set on the side wall near the bottom of cylinder. The contact between the gauge and the sand column is made of a fine mesh. As the sands to be used are initially air-dried, the measurement by such a gauge is possible till a wetting front reaches this measurement point.

Experiments are carried out, till a wetting front reaches the bottom of a sand column in an air conditioned room at about 21°C in order to prevent the physical properies, surface tension, viscosity, etc., of penetrating water from changing by a variation in temperature.

2.2 Experimental results

(1) Infiltration at the early stage

(a) pore-air pressure

The changes of pore-air pressure during a relatively early stage after the beginning of experiment are shown in **Fig. 2**(**a**) and (**b**), where an ordinate represents the quantity which is subtracted the ponding depth, h_w, from the observed pore-air pressure, p_{aL}. L is the height of sand column, that is, the thickness of sand layer. From these figures and the observation with respect to the state of escape of air from the sand surface during experiments, it can be considered that the curves showing the change of pore-air pressure with time are composed of the following two phases:

① the first phase which shows the rapid increase just after the beginning of

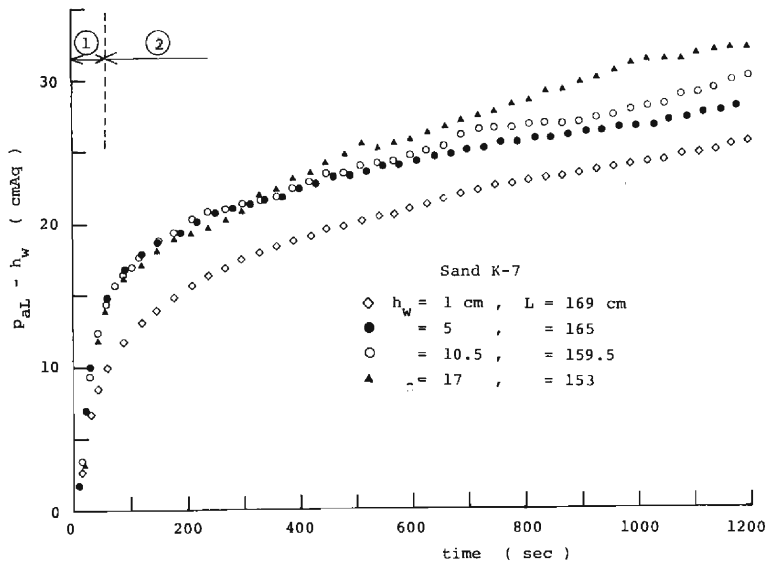

(a)

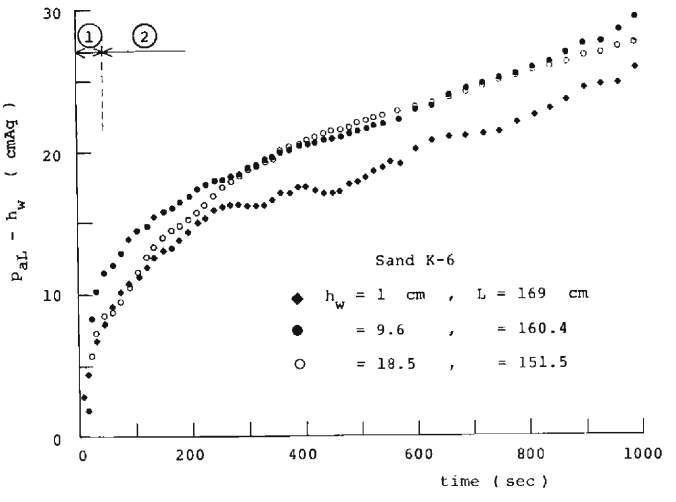

(b)

Fig. 2. Changes of pore-air pressure with time.
(a) Sand K-7
(b) Sand K-6

infiltration, and where there is only a slight escape of air from the sand surface,

② the second phase which shows a moderate increase as the rate of increase becomes lower with time, and where air escapes vigorously with a lot of small bubbles at the beginning of this phase and then the bubble activity slows down continuously to some extent with time.

As the thicknesses of the layers in the experiments described in **Fig. 2**(**a**) and (**b**)

are roughly equal, it seems from the approximate coincidence of the plotted curves that the ponding depth on the sand surface continues to act statically on the pore-air not including the time just after the beginning of experiment.

i) the effect of thickness of layer on pore-air pressure

The results of measurement in such cases where the ponding depths are same and the thicknesses of layer are different are shown in **Fig. 3**. It seems from this figure that the pore-air pressure becomes large as the layer is reduced in thickness. And, considering that the results of experiments show a certain degree of scattering under same experimental condition, it can be considered that this effect is not so great. However, the curve for $L=34$ cm differs greatly from the one for $L=59$ cm. It is known from a numerical simulation where attention was paid to the effect o the thickness of layer on pore-air that at least this great difference is not caused by the difference of the thickness of layer[16].

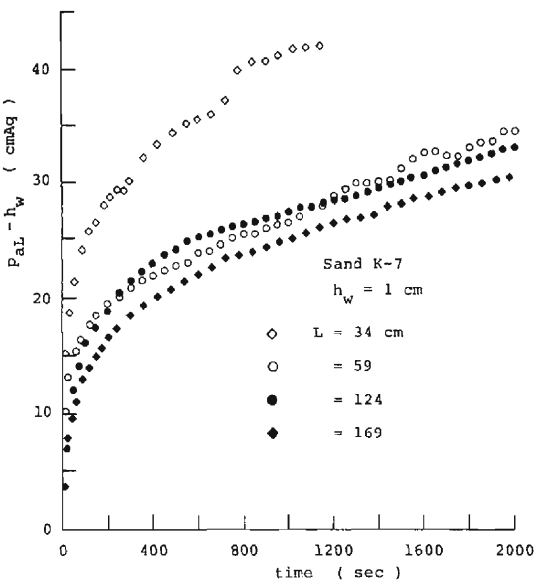

Fig. 3. Effect of the thickness of layer on pore-air pressure, in the case of Sand K-7.

ii) the change of pore-air pressure with time

Plotting the value of pore-air pressure subtracting the value of the ponding depth, in **Fig. 2** and **Fig. 3**, to the logarithmic scale of time, **Fig. 4** (**a**), (**b**) and **Fig. 5** are obtained. It is obvious that the pore-air pressure largely obeys the broken line described in the figure, excluding some duration after the beginning of infiltration, or phase ①. We express this line as

$$p_{aL} = a \ln t + b + h_w \qquad (1)$$

where a and b are numerical constants. **Table 1** is the summary of the obtained

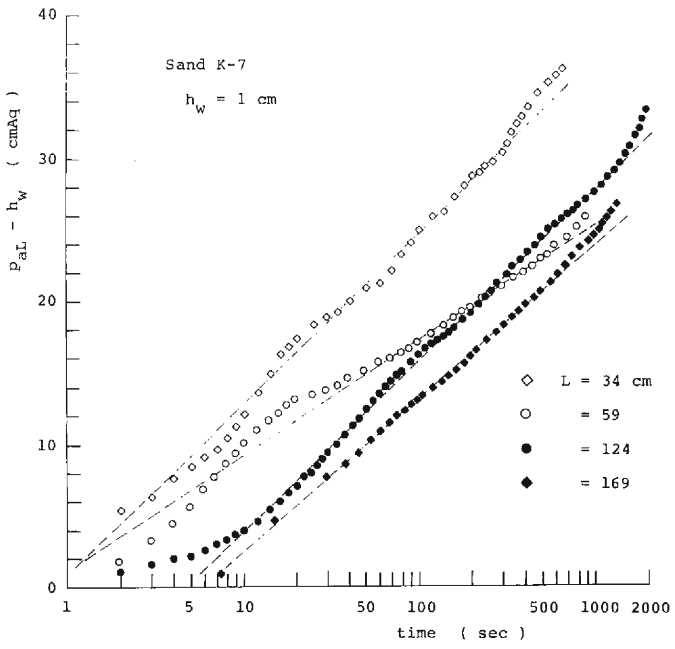

(a)

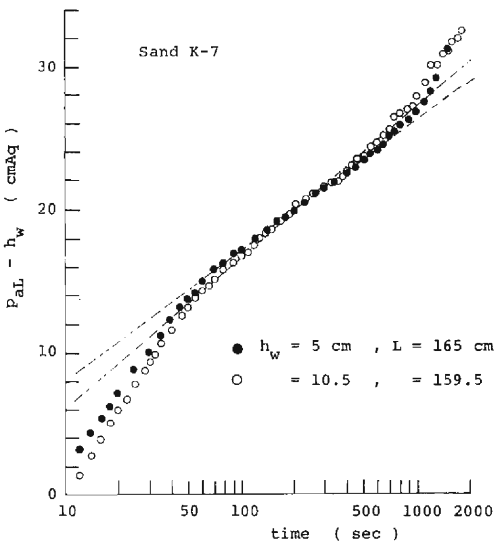

(b)

Fig. 4. Changes of pore-air pressure with a common logarithm of elapsed time, in the case of Sand K-7.
(a) $h_w = 1$ cm
(b) $h_w > 1$ cm

Table 1 Experimental constants at the early stage.

Sand	h_w	L	S	a	b	t_e	t'_e	φ
	cm	cm	cm·sec$^{-1/2}$	cmAq	cmAq	sec	sec	cm·sec$^{-1/2}$
Sand K-7	1	169	0.20	5.6	−12.8	1250	1200	0.76
	1	169	0.38	3.4	−5.3	>960	>960	1.01
	1	169	0.45	3.7	−8.0	420	360	1.02
	1	169	0.46	4.3	−8.6	700	550	1.03
	1	169	0.46	3.1	−3.9	>400	>400	1.00
	1	169	0.42	4.3	−6.2	260	260	1.12
	1	169	0.46	4.9	−8.5	600	700	1.02
	1	169	0.42	6.2	−14.0	840	800	0.96
	1	169	0.44	3.5	−5.1	660	420	1.01
	* 1	169	0.29	3.5	−3.9	1440	800	0.86
	1	169	0.29	3.9	−6.3	110	250	0.82
	1	169	0.28	3.1	−4.7	340	530	0.81
	* 1	169	0.42	4.7	−9.7	600	520	0.90
	1	169	0.33	4.1	−6.0	350	360	0.78
	1	169	0.26	5.5	−12.0	400	400	0.82
	1	129	0.32	9.9	−32.8	1100	1020	0.95
	° 1	124	0.35	5.1	−8.7	1350	700	0.87
	1	84	0.33	7.2	−16.4	960	900	0.99
	1	59	0.36	3.2	2.1	560	450	0.87
	1	59	0.27	7.9	−21.2	1700	840	0.94
	1	34	0.36	5.0	1.8	300	330	0.88
	* 5	165	0.36	3.9	−0.9	650	550	0.80
	° 5	125	0.38	7.3	−17.1	500	530	0.87
	°10	120	0.37	8.4	−18.3	450	320	0.98
	*10.5	159.5	0.33	4.6	−4.7	950	780	0.83
	*17	153	0.38	3.7	−0.5	280		0.89
	18	152	0.29	5.2	−12.9	400	480	
	*18	152	0.41	4.7	−14.1	1000	960	1.04
Sand K-6	* 1	169	0.62	3.8	−6.1	500	380	1.30
	1	169	0.53	5.0	−9.8	720	680	1.15
	1	169	0.54	5.6	−9.5	1050		1.17
	1	169	0.53	5.6	−13.1	450	440	1.15
	1	169	0.57	4.5	−9.0	400	340	1.27
	1	169	0.66	2.5	1.0	210	220	1.38
	1	169	0.66	2.5	−0.3	150	170	1.47
	* 9.6	160.4	0.54	4.6	−6.4	550	440	1.20
	*18.5	151.5	0.73	6.4	−17.9	700	480	1.55

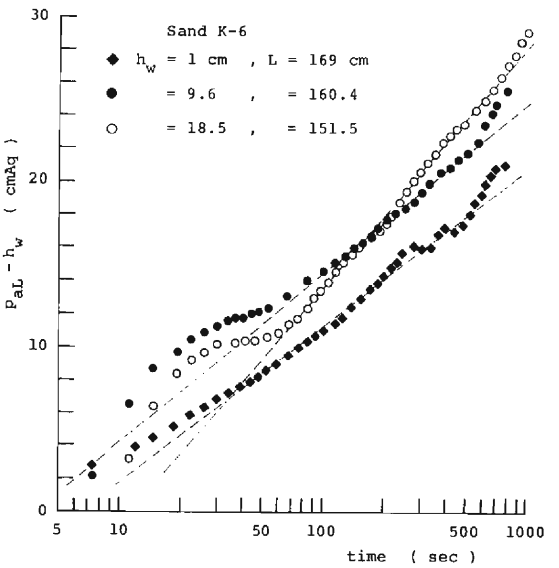

Fig. 5. Same as Fig. 4, but in the case of Sand K-6.

values of a, b and t_e which represents the time when observed pore-air pressure begins to separate from the relation given by Eq. (1), or phase ②. The value of a is 3∼10 cmAq (almost less than 6 cmAq) in Sand K-7 and 2.5∼6.5 cmAq in Sand K-6. It seems in **Table 1** that the value of a is not affected much by the particle size or the pore size, the thickness of layer, and the ponding depth. The relations between the value of pore-air pressure subtracting the value of ponding depth at $t=t_e$ and the value of a are shown in **Fig. 6** (**a**) and (**b**), where the cases of $h_w=1$ cm

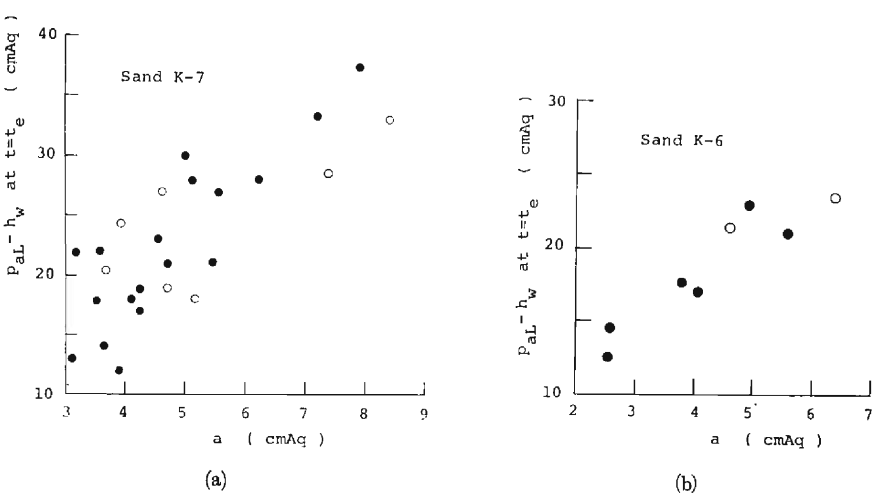

(a) (b)

Fig. 6. Relation between the value of $p_{aL}-h_w$ at $t=t_e$ and that of a.
(a) Sand K-7
(b) Sand K-6

and $h_w > 1$ cm are represented by a black circle and a white circle, respectively. It is seen from these figures that the pore-air pressure has a tendency to become large as the value of a increases and is 20～30 cmAq for Sand K-7 and 15～20 cmAq for Sand K-6, not being influenced very much by the ponding depth nor the thickness of a layer. However, the time elapsed till the observed pore-air pressure obeys

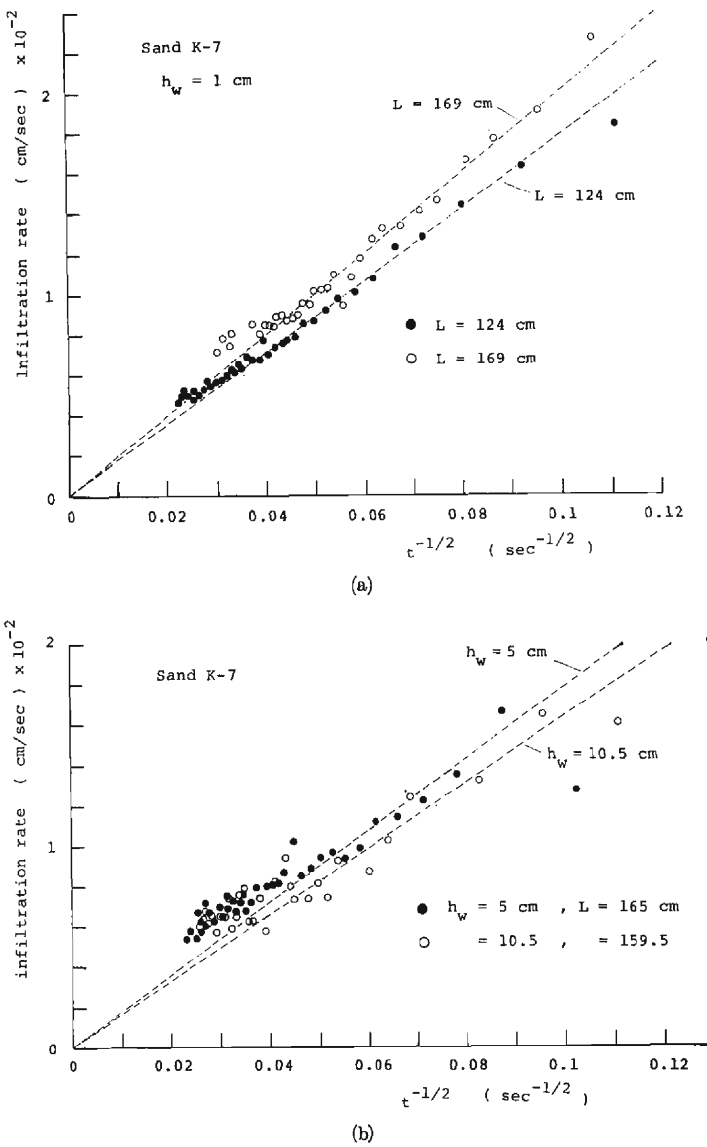

Fig. 7. Changes of infiltration rate with a inversed square root of elapsed time in the case of Sand K-7.
(a) $h_w = 1$ cm
(b) $h_w > 1$ cm

Eq. (1) increases as the ponding depth increases. This is considered to occur because practically it takes some time, according as the ponding depth increases, to fill it up the intended ponding depth with water, and because the rapidly deepening pond acts slowly on pore-air.

(b) infiltration rate

The relation between the infiltration rate and the inverse of the square root of time elapsed for Sand K-7 is shown in **Fig. 7** (**a**) and (**b**). These correspond to **Fig. 2** (**a**) and **Fig. 3**. The relation between the cumulative infiltration amount and the square root of time elapsed for Sand K-6 is shown in **Fig. 8**, corresponding to **Fig. 2** (**b**). From these figures, the following equation is given approximately, excluding the short duration after an infiltration begins, or phase ①.

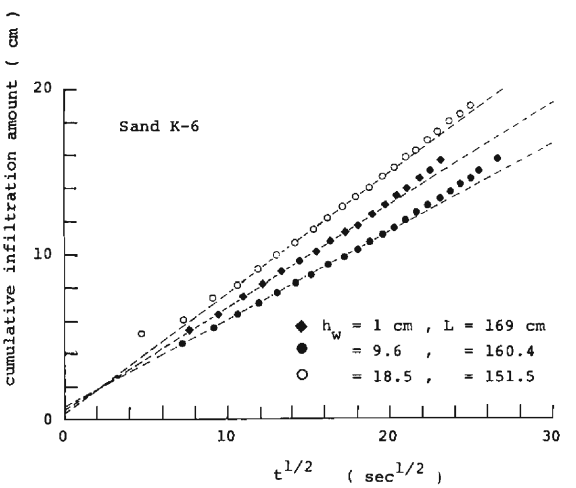

Fig. 8. Changes of cumulative amount of infiltration with a square root of elapsed time, in the case of Sand K-6.

$$f = \frac{S}{2} t^{-1/2} \tag{2}$$

$$I = St^{1/2} \tag{3}$$

where f is the infiltration rate, I the cumulative infiltration amount and S the experimental constant. Because dI/dt is equal to f, Eq. (2) is equivalent to Eq. (3). The values of S and t_e' which represents the time when the observed value begins to separate from Eq. (2) or Eq. (3), are summarized in the previous **Table 1**. The value of S is 0.2~0.46 cm/$sec^{1/2}$ for Sand K-7 and 0.53~0.73 cm/$sec^{1/2}$ for Sand K-6. But the dependance of S on layer thickness and on ponding depth is not clear. Moreover, the value of sorptivity in the case of the water pressure at the plane of infiltration being zero, introduced by Philip[17], is estimated to be 0.47 cm/$sec^{1/2}$ for Sand K-7 and 0.60 cm/$sec^{1/2}$ for Sand K-6. The value of S for Sand K-7, therefore, is less than the value of sorptivity but, for Sand K-6, the value of S is not necessarily less than the value of sorptivity.

It is obvious that the value of t_e' is nearly equal to one of t_e. This means that there is a physical correspondence between Eq. (1) and Eq. (2).

(c) moisture content

The figures of motion of penetrating water in the duration while Eq. (2) or Eq. (3) is valid, are shown in **Fig. 9** (**a**) and (**b**), where x is the depth from a sand surface and m the mass wetness, corresponding to **Fig. 7** (**a**) and **Fig. 8**, respectively.

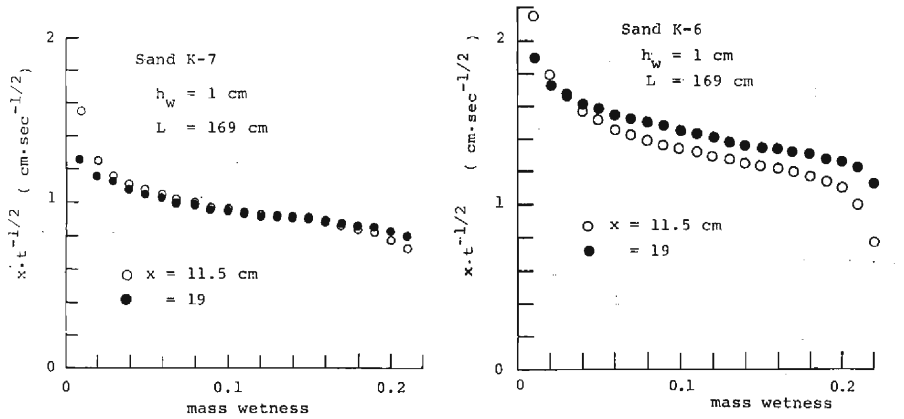

Fig. 9. Advancement of moisture.
(a) Sand K-7
(b) Sand K-6

Though the value of $x/t^{1/2}$ cannot be determined clearly because of the not-so-good accuracy of moisture measurement for $m>0.22$, it is obvious from these figures that the value of $x/t^{1/2}$ for relatively small moisture content or $m>0.22$ is nearly independent of x. So, let us express this as follows:

$$\varphi(\theta) = xt^{-1/2} \tag{4}$$

where θ is the volumetric moisture content, corresponding uniquely to the mass wetness m, and the value of φ at $m=0.15$ is shown in **Table 1**.

Let us consider that Eq. (4) is valid for the range between $\theta=0$ and $\theta=\theta_b$, where $\theta=0$ means the initial moisture content or the state of air-dried sand and θ_b is constant and maximum in the field. Then, Eq. (4) gives

$$\int_0^{\theta_b} \frac{\partial x}{\partial t} d\theta = \frac{t^{-1/2}}{2} \int_0^{\theta_b} \varphi d\theta \tag{5}$$

As the term of the left hand side is equal to an infiltration rate, comparing Eq. (5) with Eq. (2), it is seen that $\int_0^{\theta_b} \varphi d\theta$ corresponds directly to S. It can be said, therefore, that Eq. (4) includes Eq. (2) or Eq. (3) for phase ②.

(2) Infiltration at the stage after a long lapse of time

(a) infiltration rate and pore-air pressure

Owing to detailed observation under experiment, the aspect of pore-air from a sand surface is as follows: At the early stage of infiltration, the escape of air occurs as a lot of small bubbles with high frequency, corresponding to phase ② described previously. After this stage, the aspect of escape changes. The escape of air occurs repeatedly, if not so periodically. The usual pattern is one or several large bubbles and a group of small bubbles following them appear, and then the appearance of bubbles ceases. The size of large bubbles in Sand K-7 is larger than that in Sand K-6. Furthermore, the size increases with ponding depth.

The changes of infiltration rate and pore-air pressure with time till a wetting front reaches the bottom of a layer are shown in **Fig. 10** (**a**), (**b**), (**c**) and **Fig. 11**, corresponding to **Fig. 2** (**a**) and (**b**), respectively. The meaning of the broken line is stated in **6.2**. It is known from these figures that the infiltration rate and the rate of change of pore-air pressure decrease with time elapsed and approach a certain constant value, respectively. Let us represent such asymptotical values of an infiltration rate and a rate of change of pore-air pressure as f_∞ and $\dot{p}_{a\infty}$, respectively. f_∞ and $\dot{p}_{a\infty}$ for the experiment of $L=150\sim170$ cm, which is asterisked in **Table 1**, are given by **Table 2**. And as the results of measurement marked by a circle in **Table 1**, where the thickness of layer is considerably smaller than one in the above asterisked cases, show the same asymptotical characteristics, these

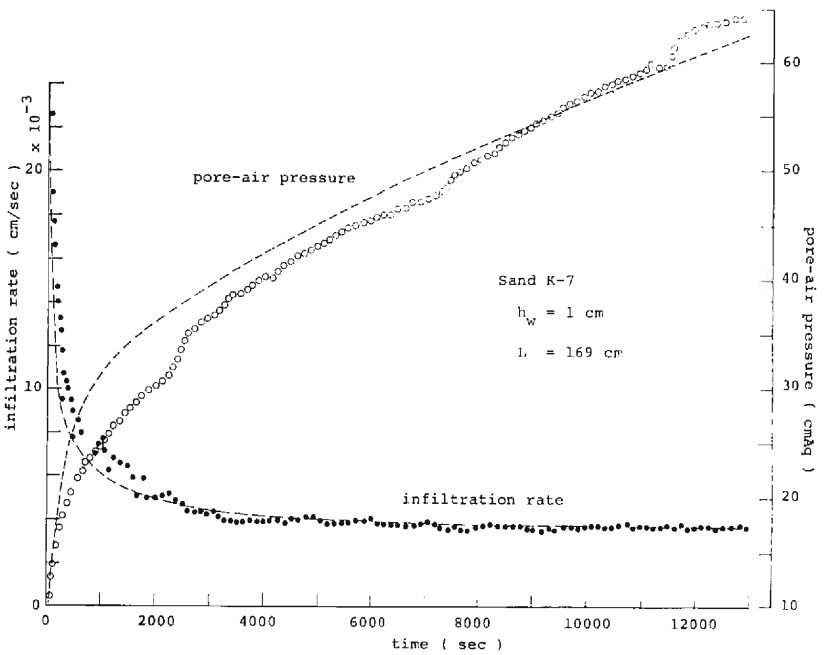

(a)

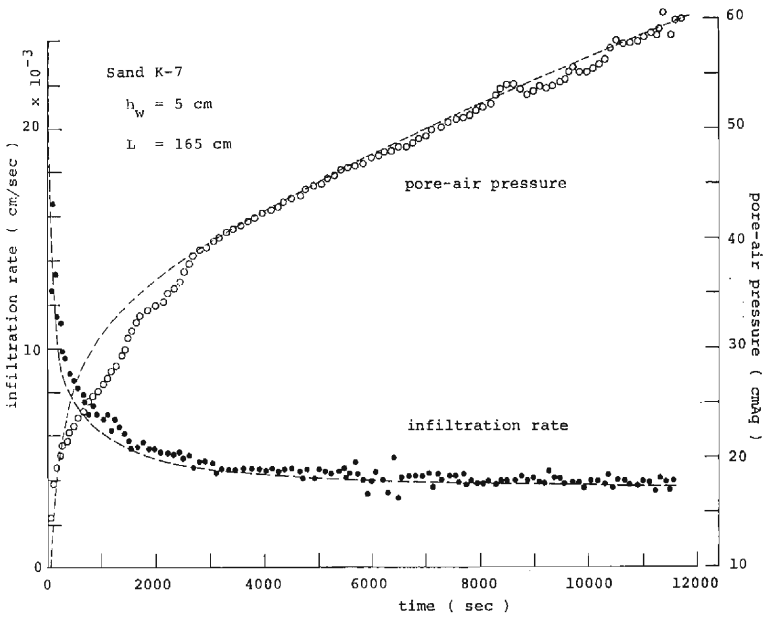

(b)

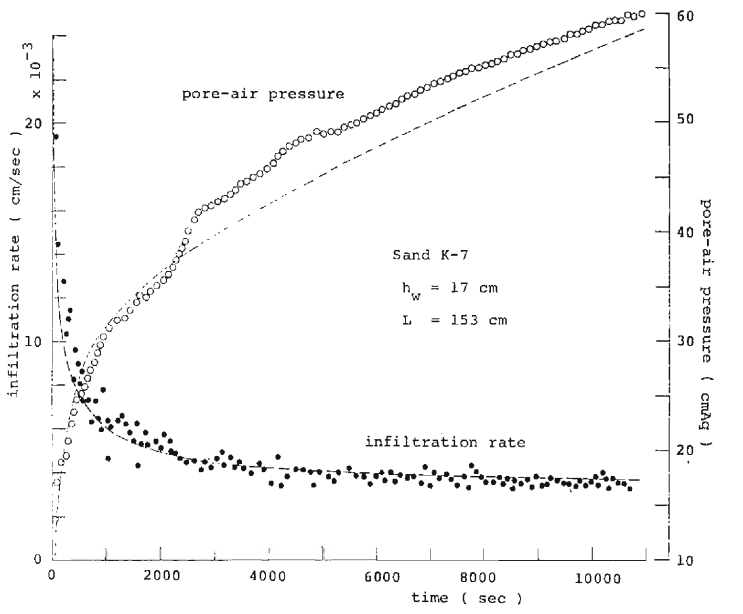

(c)

Fig. 10. Changes of infiltration rate and pore-air pressure with time, in the case of Sand K-7.
(a) h_w=1 cm, L=169 cm
(b) h_w=5 cm, L=165 cm
(c) h_w=17 cm, L=153 cm

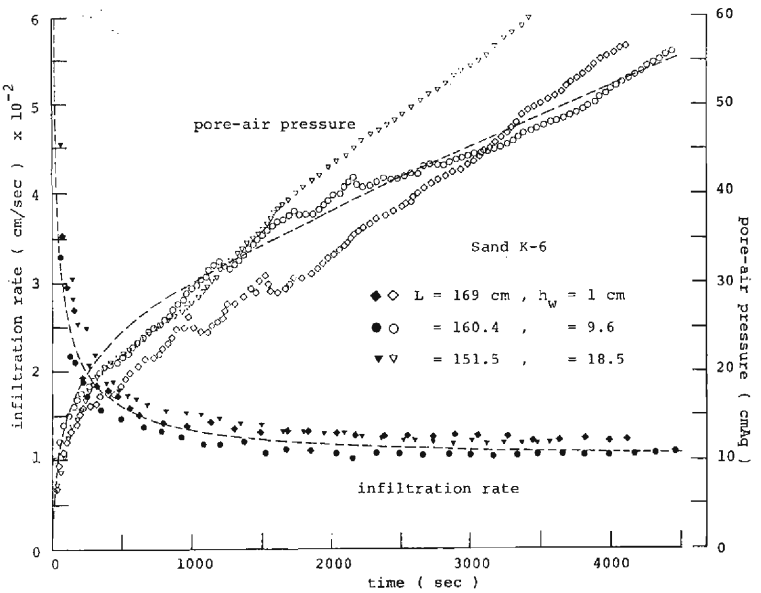

Fig. 11. Same as Fig. 10, but in the case of Sand K-6.

Table 2 Experimental constants at the stage after a long time has elapsed.

Sand	h_w	L	f_∞	$\dot{p}_{a\infty}$	ω_*	θ_*	$\theta_*\omega_*$	K_*/θ_*
	cm	cm	cm/sec $\times 10^{-3}$	cmAq/sec $\times 10^{-3}$	cm/sec $\times 10^{-2}$		cm/sec $\times 10^{-3}$	cm/sec $\times 10^{-2}$
K-7	1	169	3.7	2.75	1.06	0.38	4.0	1.15
	1	169	3.5	2.13	1.05			
	5	165	3.8	2.21	1.04	0.36	3.7	1.06
	10.5	159.5	4.0	2.80	1.09	0.38	4.1	1.15
	17	153	3.5	1.90	0.95	0.37	3.5	1.11
	18	152	2.9	4.50	0.93	0.36	3.3	1.06
	° 1	124	3.5	1.44	1.03	0.36	3.8	1.09
	° 5	125	3.2	2.20	0.93	0.36	3.3	1.06
	°10	120	2.8	1.80	0.81	0.35	2.8	1.03
K-6	1	169	12.1	11.4	2.90	0.38	10.9	2.37
	9.6	160.4	10.2	8.65	3.00	0.37	11.0	2.30
	18.5	151.5	11.9	11.5	3.16	0.37	11.7	2.30

results are also shown in **Table 2** by a circle. In **Table 2**, though the f_∞ in the cases of Sand K-7 of $h_w=10$ cm and 18 cm become somewhat smaller than the others of Sand K-7, it is obvious that the f_∞ is nearly constant for each sand and it is independent of the ponding depth. Though there are a few exceptional cases, $\dot{p}_{a\infty}$ has similar properties to f_∞. Moreover, f_∞ and $\dot{p}_{a\infty}$ for Sand K-7 is smaller than ones for Sand K-6. That is, f_∞ and $\dot{p}_{a\infty}$ decrease as the particle size of layer decrease.

Owing to our experiments of the unconfined infiltration with $h_w=1$ cm, that

is, the infiltration on a sand column with not solid but screen bed, the value corresponding to f_∞ was 6.5×10^{-3} cm/sec for Sand K-7 and 2.5×10^{-2} cm/sec for Sand K-6. Therefore, the value of f_∞ for the confined infiltration is known to be half of that for the unconfined infiltration.

Though an infiltration phenomenon is, strictly speaking, discontinuous, the characteristics obtained here suggest that the phenomena may be considered continuous in average, and the value of f_∞ and $\dot{p}_{a\infty}$ are determined by the physical properties of layer.

(b) moisture content

The change of moisture profile with time are shown in **Fig. 12** (**a**) and (**b**),

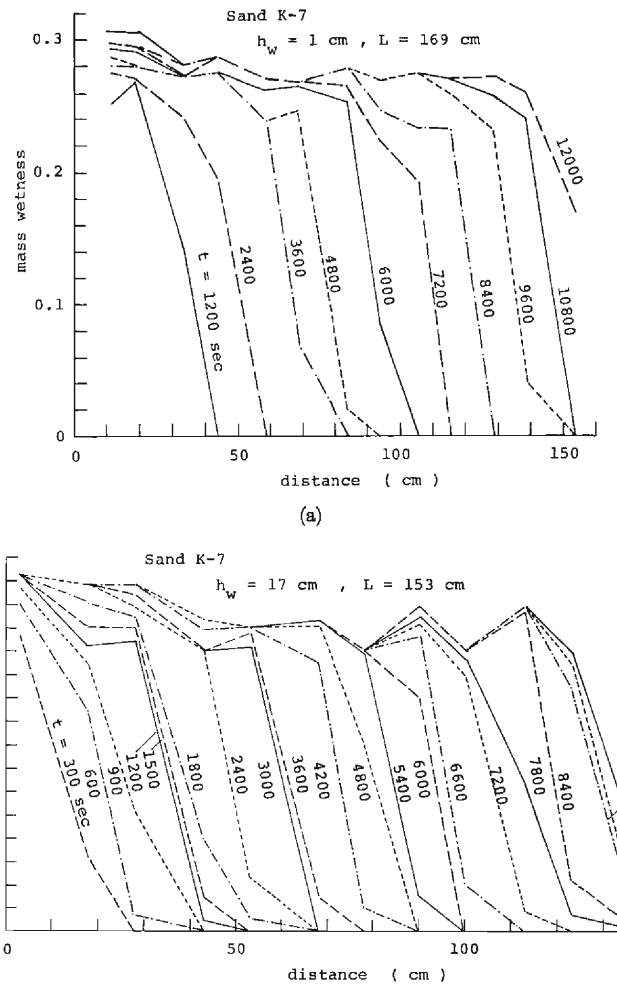

Fig. 12. Change of moisture profile with time, in the case of Sand K-7.
(a) $h_w=1$ cm, $L=169$ cm
(b) $h_w=17$ cm, $L=153$ cm

and **Fig. 13** (**a**) and (**b**), corresponding to **Fig. 10** and **Fig. 11**, respectively. From these figures and the results of other cases, the following can be seen. At the early stage of infiltration, the moisture profile is composed of the nearly saturated zone which develops downwards from a sand surface and the wetting front ahead of it. And as time goes by, the moisture profile becomes to be composed of four zones. In order from surface to bottom, the first is the above mentioned nearly saturated zone which develops downwards. The second is the transitional zone which links up the first zone at its upper boundary. The third is such a zone that moisture content is almost constant and relatively low, which develops remarkably by the advancement of the wetting front. The fourth is the wetting front which is ahead of the third zone. Then, let us call the first zone as "quasi-saturated zone" and the other zones as "unsaturated zone".

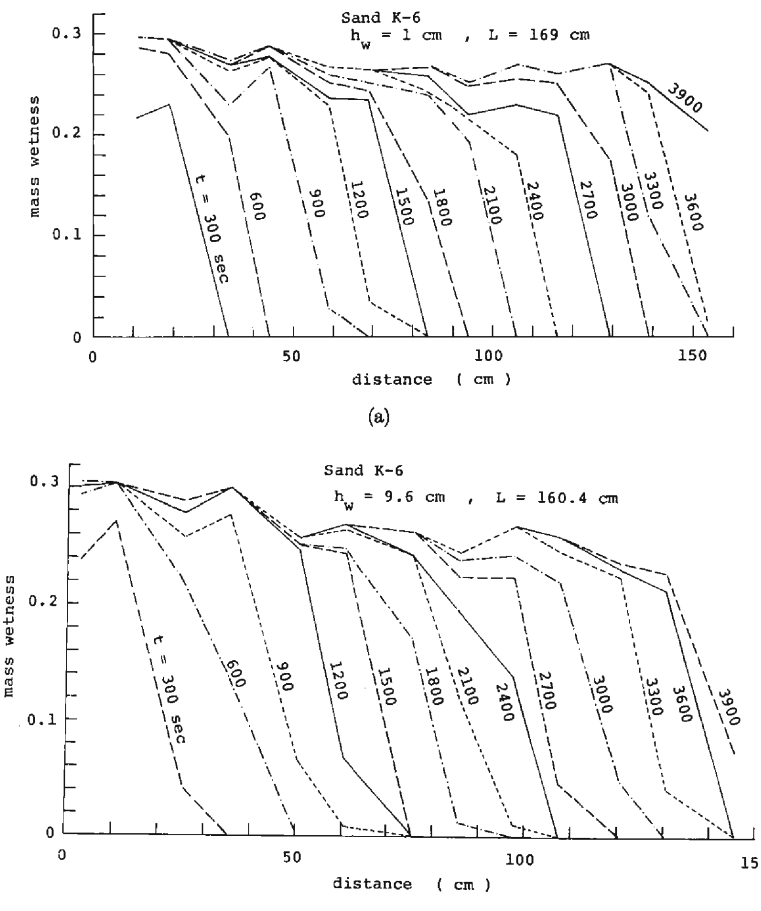

Fig. 13. Same as Fig. 12, but in the case of Sand K-6.
(a) h_w=1 cm, L=169 cm
(b) h_w=9.6 cm, L=160.4 cm

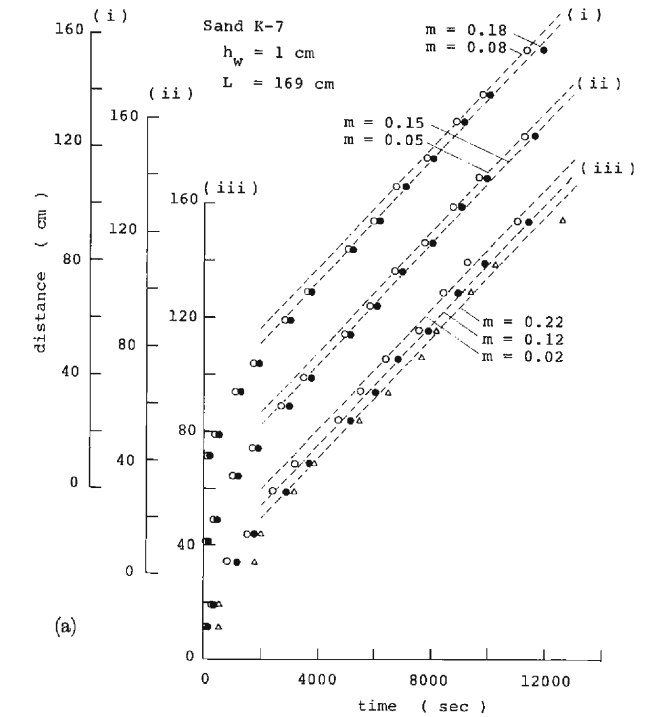

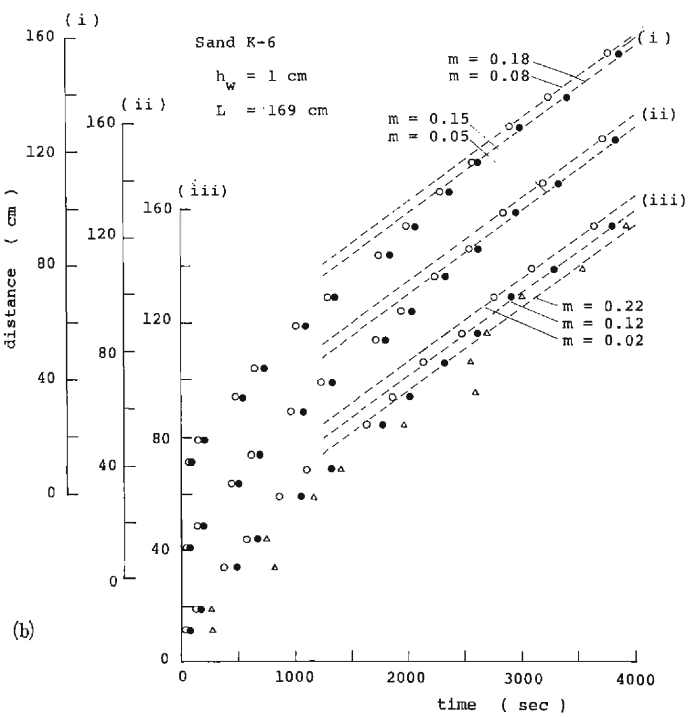

Fig. 14. Movement of wetting front.
(a) Sand K-7
(b) Sand K-6

The movement of the wetting front is shown in **Fig. 14** (**a**) and (**b**), by taking a constant moisture content as a parameter, corresponding to **Fig. 12** (**a**) and **Fig. 13** (**a**), respectively. From these figures, it is known that, as the time proceeds, the celerity of advancement of a constant moisture content decreases and approaches a nearly constant value which is given by the gradient of the broken line shown in the figures, and it seems to be independent of a moisture content. Considering both this property and the asymptotic characteristics of infiltration rate mentioned in (a), it becomes obvious that, as the time goes, the wetting front advances downwards with a constant velocity and an unchangeable profile. The third zone where moisture content remains nearly constant is called "transmission zone" in this paper.

Let us represent this constant velocity of wetting front as ω_* and the moisture content in the transmission zone as θ_*. The values of ω_* and θ_* are given in **Table 2**. Though there are a few exceptional cases in Sand K-7, it is known that both ω_* and θ_* become nearly equal for each sand. Therefore, these values are considered to be determined uniquely by the physical properties of layer.

Moreover, the value of $\theta_*\omega_*$ is nearly equal to that of f_∞ in **Table 2**. This roughly means that penetrating water from the sand surface apparently contributes to the advancement of the wetting front and that the moisture profile in the zone above the transmission zone is almost unchangeable.

3. Fundamental equations

Though the infiltration phenomenon, strictly speaking, is discontinuous, one may consider the infiltration phenomenon as a continuous process in average. Then, let us apply such a well-worn way that the appropriate average scales of time and space which are at least larger than the Darcy's scale are introduced and further that the scales are treated to be infinitesimal in mathematical expressions.

3.1 Unsaturated zone

Let us assume that both the penetrating water and the pore-air in the unsaturated zone obey the generalized Darcy's law. Under the conditions that the porous medium is homogeneous and isotropic and that the physical properties of the porous medium remain unchangeable in time and space, the equations of motion for the water and the pore-air are given as follows, respectively:

$$v = -K\left(\frac{\partial p_w}{\partial x} - 1\right) \tag{6}$$

$$v_a = -K_a\left(\frac{\partial p_a}{\partial x} - \frac{\rho_a}{\rho_w}\right) \tag{7}$$

where v is the filter velocity of water, v_a the filter velocity of pore-air, K the hydraulic conductivity, K_a the permeability of pore-air, p_w the water pressure head, p_a the air pressure in water head which is the quantity of increase over the atmos-

pheric pressure, ρ_w the density of water, ρ_a the density of pore-air, and x the vertical co-ordinate being positive in a gravitational direction and having an origin on the sand surface. Let us rewrite p_w in Eq. (6) by using p_a at the same time and position as p_w.

$$p_w = \psi + p_a \tag{8}$$

and

$$\psi = p_w - p_a \tag{9}$$

where ψ corresponds to the usual capillary potential in water head. Substituting Eq. (8) into Eq. (6) yields

$$v = -D\frac{\partial\theta}{\partial x} + K\left(1 - \frac{\partial p_a}{\partial x}\right) \tag{10}$$

where

$$D(\theta) = K\frac{d\psi}{d\theta} \tag{11}$$

ψ is assumed to be determined uniquely by θ only and D is called the moisture diffusivity.

The equations of continuity for water and pore-air are given by,

$$\frac{\partial\theta}{\partial t} + \frac{\partial v}{\partial x} = 0 \tag{12}$$

and

$$\frac{\partial\rho_a(\theta_s - \theta)}{\partial t} + \frac{\partial\rho_a v_a}{\partial x} = 0\,, \tag{13}$$

respectively, where θ_s is the volumetric moisture content in saturation. Inserting Eq. (10) into Eq. (12) and Eq. (7) into Eq. (13) yield,

$$\frac{\partial\theta}{\partial t} = \frac{\partial}{\partial x}\left\{D\frac{\partial\theta}{\partial x} - K\left(1 - \frac{\partial p_a}{\partial x}\right)\right\} \tag{14}$$

and

$$\frac{\partial\rho_a(\theta_s - \theta)}{\partial t} = \frac{\partial}{\partial x}\left\{\rho_a K_a\left(\frac{\partial p_a}{\partial x} - \frac{\rho_a}{\rho_w}\right)\right\}, \tag{15}$$

respectively.

Assuming that the pore-air is a perfect gas and changes in the isothermal process, the equation of state of pore-air becomes

$$\rho_a = C(P_{a0} + p_a) = CP_a \tag{16}$$

where C is a numerical constant, P_{a0} the pressure of atmosphere and $P_a = P_{a0} + p_a$.

After all, Eq. (14) to Eq. (16) are the fundamental equations for the unsaturated zone.

3.2 Quasi-saturated zone[18),19)]

The pore-air in the quasi-saturated zone, connecting continuously with the

air in the transitional and unsaturated zone, exists throughout that zone only when the air is escaping from the sand surface. And even when the air does not escape, the part filled with only water in the quasi-saturated zone is developing downwards in average. However, from a microscopic viewpoint, considering the fact that in the experiment using a U-shaped tube (see **Appendix**) the lower end of fluid column in the pipe of d_2 continues to move up and down, it is considered that the thickness of the part with only water increases with time in average even while fluctuating to some extent. In spite of such a complicated behaviour of air, it is possible to treat the water in the quasi-saturated zone as moving downwards in average. Therefore, let us assume that the water in the quasi-saturated zone obeys the following equation, being similar to Darcy's law.

$$\hat{v} = \hat{K}\left(1-\frac{p_{w1}-p_{w0}}{x_1}\right), \quad \hat{v}=f \tag{17}$$

where $\hat{v}$ is the filter velocity of water, $\hat{K}$ the equivalent hydraulic conductivity, x_1 the thickness of the quasi-saturated zone, p_{w0} the water pressure head at $x=0$, and p_{w1} the water pressure head at $x=x_1$. And it is assumed that the distribution of moisture content in the quasi-saturated zone is uniform. Therefore, $\hat{v}$ becomes equal to the infiltration rate f. Let us rewrite p_{w1} by using p_{a1} which is the air pressure at $x=x_1$ as follows:

$$p_{w1} = \psi_1 + p_{a1} \tag{18}$$

and

$$\psi_1 = p_{w1} - p_{a1} \tag{19}$$

where p_{a1} and p_{w1} are defined at same time. Inserting Eq. (18) into Eq. (17) yields

$$f = \hat{v} = \hat{K}\cdot\left(1-\frac{\psi_1+p_{a1}-p_{w0}}{x_1}\right) \tag{20}$$

On the other hand, though the behavior of existing air in the quasi-saturated zone is very complicated, it is obvious that the air moves upwards in average. So, let us assume that the air moves continuously in average and the motion of air obeys approximately the following equation, being similar to the equation of motion of water Eq. (20).

$$\hat{v}_a = -\hat{K}_a\cdot\frac{p_{a1}-p_{a0}}{x_1} \tag{21}$$

where $\hat{v}_a$ is the filter velocity of air and has a negative sign, $\hat{K}_a$ the equivalent permeability of air, and p_{a0} the air pressure in water head at $x=0$.

Eq. (20) and Eq. (21) are the fundamental equations for the quasi-saturated zone. For the convenience of analysis, let us transform these equations. That is, first we introduce the unknown function of time, $r(t)$, as follows:

$$\hat{v}_a = -r(t)\cdot\hat{v} \tag{22}$$

Inserting Eq. (2) and Eq. (21) into the above equation yields

$$p_{a1} = (1-\alpha_r)x_1-(1-\alpha_r)\psi_1+p_{w0}+\alpha_r(p_{a0}-p_{w0}) \tag{23}$$

or

$$p_{a1} = (1-\alpha_r)x_1-\psi_1+p_{w0}-\beta_r \tag{24}$$

where

$$\alpha_r = \frac{\hat{K}_a}{\hat{K}_a+r\hat{K}} \tag{25}$$

$$\beta_r = \alpha_r(-\psi_1+p_{w0}-p_{a0}) \tag{26}$$

Substituting Eq. (24) into Eq. (20), we obtain the following equation.

$$\hat{v} = \alpha_r\hat{K}\left(1+\frac{\beta_r/\alpha_r}{x_1}\right) \tag{27}$$

Eq. (27) and Eq. (24) as the fundamental equations in stead of Eq. (20) and Eq. (21) are applied in the following analysis.

3.3 Initial and boundary conditions

As mentioned in **2.1**, the layer is made of an air-dried sand and, at the beginning of experiment, the pore-air of any layer are at atmospheric pressure. Then, the initial conditions of water and pore-air are given by,

$$\theta = \theta_0 = \text{constant} \approx 0 \tag{28}$$

$$p_a = 0\,, \tag{29}$$

respectively, where θ_0 is the moisture content of air-dried sand.

As the bottom of layer is bounded, the boundary conditions at $x=L$ for water and pore-air becomes:

$$v = 0 \tag{30}$$

$$v_a = 0\,, \tag{31}$$

respectively.

4. Several characteristics of the behaviour of water and air

4.1 The early stage of infiltration[15]

(1) Pore-air pressure

Let us examine the behaviour of pore-air pressure by using the fundamental equations given by Eq. (14) to Eq. (16) and the characteristics of the movement of water given by Eq. (4).

Let us assume that Eq. (4) is applicable to the range $(0, \theta_b)$. And for the convenience of analysis, converting independent variables (x, t) in Eq. (14) into (θ, t), it becomes:

$$-\frac{\partial x}{\partial t}=\frac{\partial}{\partial\theta}\left\{D\Big/\frac{\partial x}{\partial\theta}-K\left(1-\frac{\partial p_a}{\partial\theta}\Big/\frac{\partial x}{\partial\theta}\right)\right\} \tag{32}$$

And by the same transformation, Eq. (15), after inserting Eq. (16), becomes:

$$(\theta_s-\theta)\left(\frac{\partial p_a}{\partial t}-\frac{\partial p_a}{\partial\theta}\cdot\frac{\partial x}{\partial t}\Big/\frac{\partial x}{\partial\theta}\right)+P_a\cdot\frac{\partial x}{\partial t}\Big/\frac{\partial x}{\partial\theta}=\frac{\partial}{\partial\theta}\left(K_aP_a\cdot\frac{\partial p_a}{\partial\theta}\Big/\frac{\partial x}{\partial\theta}\right)\Big/\frac{\partial x}{\partial\theta} \tag{33}$$

where we assume that

$$\frac{\partial p_a}{\partial x}-\frac{\rho_a}{\rho_w}\approx\frac{\partial p_a}{\partial x} \tag{34}$$

because ρ_a/ρ_w is in the order of 10^{-3} and $\partial p_a/\partial x$ is considered to be much larger than ρ_a/ρ_w, excluding the domain where the moisture content is very small. Even with a small moisture content, the assumption of Eq. (34) does not become a serious problem as shown in the next induction.

Applying the relation of Eq. (4) to Eq. (32), we obtain

$$-\frac{t^{-1/2}}{2}\varphi=t^{-1/2}\frac{d}{d\theta}(D/\varphi')-\frac{\partial}{\partial\theta}\left[K\left\{1-\frac{\partial p_a}{\partial\theta}\Big/(\varphi' t^{1/2})\right\}\right] \tag{35}$$

where in the transformation, the following relations are used.

$$\frac{\partial x}{\partial\theta}=\varphi' t^{1/2},\quad \frac{\partial x}{\partial t}=\frac{\varphi}{2}t^{-1/2} \tag{36}$$

where the prime means the differential operator with respect to θ.

By considering the initial condition Eq. (28) and the boundary condition Eq. (30), the following equations can be considered to be valid at $\theta\to\theta_0$.

$$1\Big/\frac{\partial x}{\partial\theta}\to 0 \tag{37}$$

$$v\to 0 \tag{38}$$

Integrating Eq. (35) and considering the boundary conditions, Eq. (37) and Eq. (38) yield

$$\frac{\partial p_a}{\partial\theta}=H\varphi'+t^{1/2}\varphi' y \tag{39}$$

where
$$H(\theta)=-\left\{\int_0^\theta\varphi d\theta+D/\varphi'\right\}\Big/K \tag{40}$$

$$y(\theta)=\{K(\theta)-K(\theta_0)\}/K(\theta) \tag{41}$$

and y corresponds to the gravitational term in the generalized Darcy's law for water Eq. (10). Dividing both sides of Eq. (39) by $\partial x/\partial\theta$ given in Eq. (36), we get

$$\frac{\partial p_a}{\partial \theta}\Big/\frac{\partial x}{\partial \theta} = \left(\frac{\partial p_a}{\partial x}\right)_t = t^{-1/2}H + y \tag{42}$$

Next, substituting the relation of Eq. (4) into Eq. (33) yields

$$\frac{\partial p_a}{\partial t} - \frac{t^{-1}}{2}\frac{\varphi}{\varphi'}\frac{\partial p_a}{\partial \theta} = -t^{-1}\frac{G_1(\theta, t)}{\theta_s - \theta} \tag{43}$$

where

$$G_1 = \frac{P_a}{2}\frac{\varphi}{\varphi'} - \frac{P_a}{\varphi'}\left(\frac{dK_aH}{d\theta} + t^{1/2}y\frac{dK_a}{d\theta}\right) - K_aH^2\left(1 + y\frac{t^{1/2}}{H}\right)^2 \tag{44}$$

As we are focusing on the early stage of infiltration, it will be possible to assume that the gravity term K in the equation of motion of water, Eq. (1), is negligibly small compared with the diffusive term $\left|D\frac{\partial \theta}{\partial x}\right|$. As the relation, $\left|D\frac{\partial \theta}{\partial x}\right| \gg K$, is equivalent to ignore the term of y in the above mentioned equations, Eqs. (39), (42) and (44) become:

$$\frac{\partial p_a}{\partial \theta} = H\varphi' \tag{45}$$

$$\frac{\partial p_a}{\partial \theta}\Big/\frac{\partial x}{\partial \theta} = t^{-1/2}H \tag{46}$$

$$\{G_1\}_{y\to 0} \equiv G(\theta) = \frac{P_{a0}}{2}\frac{\varphi}{\varphi'} - \frac{P_{a0}}{\varphi'}\frac{dK_aH}{d\theta} - K_aH^2, \tag{47}$$

respectively, where, as it can be considered that $P_{a0} \gg p_a$, P_a is approximated by P_{a0}. Moreover, inserting Eq. (47) into Eq. (43), we obtain

$$\frac{\partial p_a}{\partial t} = t^{-1}\left(\frac{1}{2}\varphi H - \frac{G}{\theta_s - \theta}\right) \tag{48}$$

Now, as the right side term of Eq. (45) is the function of only θ, p_a can be expressed by the sum of the function of θ and the function of t. From this, Eq. (48) becomes:

$$\frac{\partial p_a}{\partial t} = \gamma t^{-1} \tag{49}$$

where

$$\gamma = \frac{1}{2}\varphi_b H_b - \frac{G_b}{\theta_s - \theta_b} = \text{constant}. \tag{50}$$

γ is defined at $\theta = \theta_{b-}$ and the subscript b means the value at $\theta = \theta_{b-}$. Integrating Eq. (49) with respect to t, we get

$$p_a(\theta, t) = \gamma \ln t - \gamma \ln t_i + p_a(\theta, t_i) \tag{51}$$

where t_i is a certain constant, being less than t under consideration. As it can be assumed that the pore-air pressure at $\theta \approx \theta_0$ is nearly equal to that at the bottom

of layer which is measured directly in the experiments, p_{aL}, we get the following equation from Eq. (51).

$$p_{aL}(t) = \gamma \ln t - \gamma \ln t_i + p_{aL}(t_i) \tag{52}$$

It is obvious that Eq. (52) is similar to Eq. (1) obtained by the experiments. So, comparing Eq. (52) with Eq. (1), it is known that the experimental constants a and b correspond to γ and $-\gamma \ln t_i + p_{aL}(t_i) - h_w$, respectively. After all, under the assumption $\left|D\frac{\partial\theta}{\partial x}\right| \gg K$, when the fundamental equations have the solution $x=\varphi t^{1/2}$, that is, the so-called similarity solution, it is found out that the change of the observed pore-air pressure with time, which is nearly equal to the air pressure ahead of the wetting front, is to be shown by the logarithmic function of time expressed by Eq. (1) or Eq. (52). This result inevitablely shows that t_e becomes approximately equal to t_e' in the experiments.

Integrating Eq. (45) with respect to θ yields

$$p_a(\theta, t) = p_a(\theta_{b\_}, t) + \int_{\theta}^{\theta_b} H\varphi' d\theta \tag{53}$$

In this equation, $p_a(\theta, t) - p_a(\theta_{b\_}, t) \equiv \Delta p_{ab}$, the pore-air pressure relative to that at $\theta=\theta_{b\_}$, becomes the function of only θ. Δp_{ab} can then be expressed by the similarity solution as $xt^{-1/2}$. If $p_a(\theta_{b\_}, t)$ is constant, the pore-air pressure at the point having a constant moisture content becomes constant, *i.e.*, independent of time. However, as we observed in experiments, the pore-air pressure continues to increase as time goes by. Therefore, $p_a(\theta_{b\_}, t)$, that is, the pore-air pressure at the lower end of the quasi-saturated zone can be considered to increase as the logarithmic function of time.

(2) Relation between S and γ

Under the condition of $\left|D\frac{\partial\theta}{\partial x}\right| \gg K$, Eq. (10) is rewritten as

$$v = -D(1-\tilde{A}) \Big/ \frac{\partial x}{\partial \theta} \tag{54}$$

where

$$\tilde{A} = -\frac{K}{D}\left(\frac{\partial p_a}{\partial \theta} \Big/ \frac{\partial x}{\partial \theta}\right)\frac{\partial x}{\partial \theta} = -\frac{K}{D}\frac{\partial p_a}{\partial \theta} \tag{55}$$

And applying Eq. (36), Eq. (39) and Eq. (46) to Eq. (54), we get

$$v = -t^{-1/2} D(1-\tilde{A})/\varphi' \tag{56}$$

where

$$\tilde{A} = -\frac{KH\varphi'}{D} = \frac{1}{D}\left\{\frac{\varphi'}{2}\int_0^{\theta} \varphi d\theta + D\right\} \tag{57}$$

It can be found out that, from Eq. (57), $\tilde{A}$ is the function of only θ and that, from Eq. (54), $1>\tilde{A}>0$ because v is positive and $\partial x/\partial\theta$ is negative.

Under the condition of Eq. (34), Eq. (7) can be rewritten by using Eq. (36), Eq. (40) and Eq. (46) as

$$v_a = -t^{-1/2}K_aH = t^{-1/2}\frac{1-A}{A}\frac{\tilde{A}D}{\varphi'} \tag{58}$$

where

$$A(\theta) = \frac{K}{K+K_a} \tag{59}$$

Adding v given by Eq. (56) to v_a given by Eq. (58), we get the following equation.

$$v+v_a = -t^{1/2}V \tag{60}$$

where
$$V = -\frac{D}{\varphi'}\left(1-\frac{\tilde{A}}{A}\right) \tag{61}$$

Inserting Eq. (57) and Eq. (61) into Eq. (50) yields

$$r = \frac{\varphi_b}{4K_{ab}}(S-2V_b)+\left\{\frac{(S-2V_b)^2}{4K_{ab}}+\frac{S-2V_bA_b}{2D_b(1-A_b)}P_{a0}\left(\frac{dV}{d\theta}\right)_b\right\}\Big/(\theta_s-\theta_b) \tag{62}$$

where the subscript b is the value at $\theta=\theta_{b-}$, and

$$S = \int_0^{\theta_b}\varphi d\theta \tag{63}$$

This S means the S in Eq. (2).

In order to examine the relationship between S and r, let us compare the magnitudes of each term on the right side of Eq. (62). Firstly, it is considered that, from Eq. (60),

$$\left(\frac{dV}{d\theta}\right)_b \approx 0 \tag{64}$$

because the pore-air in the region is compressed a little. Next, it is obvious that

$$\varphi_b \ll \frac{S-2V_b}{\theta_s-\theta_b} \tag{65}$$

Eq. (62) becomes:

$$r \approx \frac{(S-2V_b)^2}{4(\theta_s-\theta_b)K_{ab}} \tag{66}$$

or

$$\frac{S^2}{4r} \approx (\theta_s-\theta_b)K_{ab}\Big/\left(1-\frac{2V_b}{S}\right)^2 \tag{67}$$

Let us express the ratio of v_a and v at $\theta=\theta_{b\_}$ as $-r(t)$.

$$(v_a)_b = -r(t)\cdot(v)_b \tag{68}$$

Inserting Eq. (68) into Eq. (62) yields

$$S-2V_b = rS \tag{69}$$

Moreover, inserting Eq. (69) into Eq. (66) yields

$$\frac{S^2}{4\gamma} \approx \frac{(\theta_s-\theta_b)K_{ab}}{r^2} \tag{70}$$

As γ means the experimental constant a in Eq. (1), in light of Eq. (70), we can get the relation between $S^2/4a$ and S as shown in **Fig. 15** (**a**) and (**b**), where the experimental values in $h_w=1$ cm are shown by a black circle and in $h_w>1$ cm by a white circle. It is known from these figures that the change of $S^2/4a$ with S can be expressed approximately as the broken line shown in the figures. $d(S^2/4a)/dS$ is positive. The following relations with respect to $\partial a/\partial S$, therefore, can be determined.

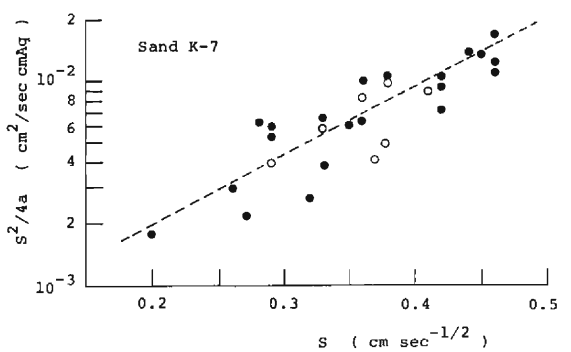

(a)

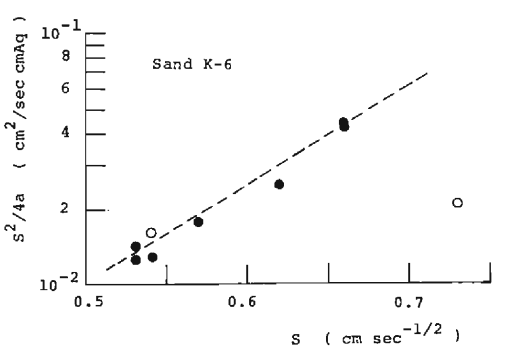

(b)

Fig. 15. Relation between $S^2/4a$ and S.
(a) Sand K-7
(b) Sand K-6

$$\frac{\partial a}{\partial S}<0 \quad \text{for } S>0.26 \text{ in Sand K-7}, \quad S>0.5 \text{ in Sand K-6}$$

$$\frac{\partial a}{\partial S}>0 \quad \text{for } S<0.26 \text{ in Sand K-7}, \quad S<0.5 \text{ in Sand K-6}$$

(3) Permeability of pore-air

In order to examine the magnitude of K_a, under the assumptions of Eq. (64) and Eq. (65), let us express the permeability of pore-air by power function of $(\theta_s-\theta)$ as[20]

$$K_a(\theta) = K(\theta_s)\frac{\mu_w}{\mu_a}\left(1-\frac{\theta}{\theta_s}\right)^{A} \tag{71}$$

where μ_w and μ_a are the coefficient of viscosity of water and air, respectively, and A a positive numerical constant. Here, if $\theta_s-\theta_b$, r and $S^2/4a$ are given, the value of A in Eq. (71) can be calculated by combination of Eq. (70) and Eq. (71). For example, putting $\theta_s-\theta_b=0.05$ under the conditions of $\theta_b=0.9\,\theta_s$ and $\theta_s=0.46$ for Sand K-7, $S^2/4a=5\times10^{-3}$ cmAq cm^2/sec from **Fig. 15** (**a**) and $r=0.7$ or 0.5, the value of A can be estimated as 1 or 1.2.

4.2 The stage after a long lapse of time[21]

Befor examining the several characteristics in the wetting front zone after a long time has elapsed, let us transform the fundamental equations and the conditions mentioned already.

As the profile and the velocity of wetting front becomes unchangeable as time goes by, we can give the approximate solution for the advancing wetting front as

$$\begin{aligned} x(\theta,\tau) &= \omega_*\tau+\zeta(\theta) \\ \tau &= t-t_0 \end{aligned} \tag{72}$$

where t_0 is the time when the above mentioned unchangeability becomes nearly valid and $\zeta(\theta)$ the moisture profile at $t=t_0$, and Eq. (72) is applicable to the range of $\theta_0<\theta<\theta_*$.

After introducing Eq. (72) into Eq. (14) and Eq. (15), using Eq. (16), we obtain the following two equations.

$$\omega_*\frac{d\theta}{d\zeta}+\frac{d}{d\zeta}\left(D\frac{d\theta}{d\zeta}+K\frac{\partial p_a}{\partial\zeta}\right)-\frac{dK}{d\theta}\frac{d\theta}{d\zeta}=0 \tag{73}$$

$$(\theta_s-\theta)\left(\frac{\partial p_a}{\partial\tau}-\omega_*\frac{\partial p_a}{\partial\zeta}\right)+P_a\omega_*\frac{d\theta}{d\zeta}=\frac{\partial}{\partial\zeta}\left\{P_aK_a\left(\frac{\partial p_a}{\partial\zeta}-\frac{\rho_a}{\rho_w}\right)\right\} \tag{74}$$

For the convenience of analysis, let us represent the value of ζ at $\theta=\theta_{*-}$ and θ_{0+} as follows:

$$\lim_{\theta\to\theta_{*-}}\zeta=\zeta_*\,,\quad \lim_{\theta\to\theta_{0+}}\zeta=\zeta_0 \tag{75}$$

Considering the characteristics of the moisture profile during infiltration and the initial condition, Eq. (28), we can put the following conditions for the water.

$$\lim_{\zeta\to\zeta_*}\frac{d\theta}{d\zeta}=0 \tag{76}$$

$$\lim_{\zeta\to\zeta_0}\frac{d\theta}{d\zeta}=0 \tag{77}$$

$$\lim_{\zeta\to\zeta_0}v=K_0\left\{1-\left(\frac{\partial p_a}{\partial\zeta}\right)_0\right\}\equiv v_0 \tag{78}$$

where the subscript 0 means the values at $\theta=\theta_{0+}$.

On the other hand, the conditions for the pore-air are as follows. Let us represent v at $\zeta=\zeta_0$ as v_{a_0}. Considering both the boundary condition, Eq. (31), and the initial condition, Eq. (28), it can be approximated that $v_{a_0}=0$. However, as it is considered physically that the upward filter velocity of air is nearly equal to the downward filter velocity of water in the front of unsaturated zone, the following expression can be described, where, of course, both v_{a_0} and v_0 are very small.

$$\lim_{\zeta\to\zeta_0}v_a=\lim_{\zeta\to\zeta_0}\left\{-K_a\left(\frac{\partial p_a}{\partial\zeta}-\frac{\rho_a}{\rho_w}\right)\right\}\equiv v_{a_0}=-v_0 \tag{79}$$

And as we cannot *a priori* give the condition for the pore-air at $\zeta=\zeta_*$, we introduce the following unknown function $u(\tau)$.

$$\lim_{\zeta\to\zeta_*}\left(\frac{\partial p_a}{\partial t}\right)_x=\lim_{\zeta\to\zeta_*}\left(\frac{\partial p_a}{\partial\tau}-\omega_*\frac{\partial p_a}{\partial\zeta}\right)=u(\tau) \tag{80}$$

(1) Celerity of wetting front

After integrating Eq. (73) with respect to ζ, using Eq. (78), we get,

$$\omega_*(\theta-\theta_0)+D\frac{d\theta}{d\zeta}+K\frac{\partial p_a}{\partial\zeta}-K+v_0=0 \tag{81}$$

Putting $\theta=\theta_{*-}$ in Eq. (81) and applying the condition Eq. (76), Eq. (81) becomes

$$\omega_*=\frac{K_*\left\{1-\left(\frac{\partial p_a}{\partial\zeta}\right)_*\right\}-v_0}{\theta_*-\theta_0} \tag{82}$$

where the subscript $*$ means the value at $\theta=\theta_{*-}$.

In order to get the expression of $(\partial p_a/\partial\zeta)_*$ in the above equation, after integrating Eq. (74) with respect to ζ, and applying the condition Eq. (78), we obtain the following relation.

$$\int_{\zeta_0}^{\zeta}(\theta_s-\theta)\left(\frac{\partial p_a}{\partial\tau}-\omega_*\frac{\partial p_a}{\partial\zeta}\right)d\zeta+P_a\omega_*(\theta-\theta_0)\approx P_a\left\{K_a\left(\frac{\partial p_a}{\partial\zeta}-\frac{\rho_a}{\rho_w}\right)+v_{a0}\right\} \tag{83}$$

where we put $P_a=P_{a_0}$, because p_a is negligibly small to P_{a0}. And Eq. (34) is also valid in this state. Moreover, when $\partial p_a/\partial\zeta-\rho_a/\rho_w\approx\partial p_a/\partial\zeta$ in Eq. (83), Eq. (83) is simplified as

$$\frac{\partial p_a}{\partial\zeta}=\frac{\theta-\theta_0}{K_a}\omega_*+\eta-\frac{v_{a0}}{K_a} \tag{84}$$

where

$$\eta=-\frac{1}{K_aP_a}\int_{\zeta}^{\zeta_0}(\theta_s-\theta)\left(\frac{\partial p_a}{\partial\tau}-\omega_*\frac{\partial p_a}{\partial\zeta}\right)d\zeta \tag{85}$$

As $-v_{a0}=v_0$ in Eq. (79), from Eq. (79) and Eq. (84), $(\partial p_a/\partial\zeta)_0$ is given by,

$$\left(\frac{\partial p_a}{\partial\zeta}\right)_0=\frac{K_0}{K_0+K_{a0}}=A_0 \tag{86}$$

Inserting Eq. (86) into the condition Eq. (78) yields

$$v_0=K_0(1-A_0) \tag{87}$$

After all, when we insert Eq. (84) at $\zeta=\zeta_*$ into Eq. (82) and use Eq. (87), we get the following equation.

$$\omega_*=\frac{K_*(1-A_*)(1-\eta_*)-K_0(1-A_0)}{\theta_*-\theta_0} \tag{88}$$

Especially in case of $|\eta_*|\ll1$, Eq. (88) is approximated by,

$$\omega_*=\frac{K_*(1-A_*)-K_0(1-A_0)}{\theta_*-\theta_0} \tag{89}$$

In order to find out the condition of existence of ω_*, inserting Eq. (84) into Eq. (81) and applying Eq. (79) and Eq. (87), we obtain

$$\frac{d\zeta}{d\theta}=-\frac{D(1-A)}{(\theta-\theta_0)\omega_*-K(1-A)+KA(K_a\eta/K)+K_0(1-A_0)} \tag{90}$$

As $d\zeta/d\theta\leq0$ and $D(1-A)>0$, we get the following conditional equation

$$\omega_*\geq\frac{K(1-A)(1-\eta)-K_0(1-A_0)}{\theta-\theta_0} \tag{91}$$

where the sign of equality is when $d\theta/d\zeta=0$ is satisfied. Especially in case of $|\eta|\ll1$, the above relation becomes

$$\omega_*\geq\frac{K(1-A)-K_0(1-A_0)}{\theta-\theta_0} \tag{92}$$

The shapes of function $K(1-A)$ and A in Sand K-7 are shown in **Fig. 16**, where the values of θ for the greatest value of $\{K(1-A)-K_0(1-A_0)\}/(\theta-\theta_0)$ and $K(1-A)$

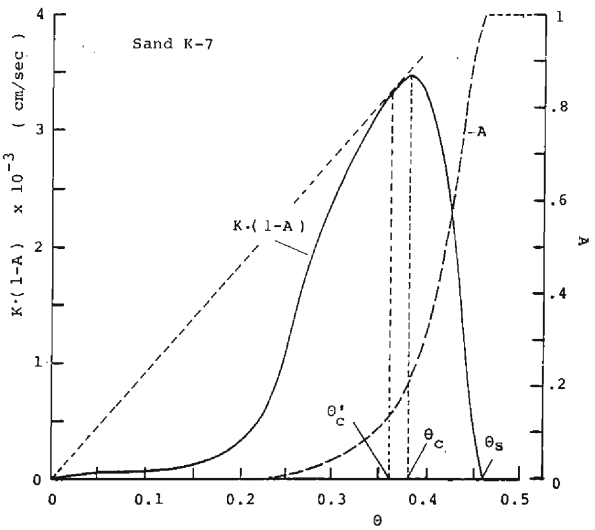

Fig. 16. Relation between $K(1-A)$ or A and moisture content θ, in the case of Sand K-7.

are represented as θ_c' and θ_c, respectively. It is known from this figure that θ_c' is a little less than θ_c, and that $\{K(1-A)-K_0(1-A_0)\}/(\theta-\theta_0)$ increases in the range of $\theta<\theta_c'$ and decreases in the range of $\theta>\theta_c'$ as the value of θ increases. These properties can be also obtained for Sand K-6. Then, when $|\eta| \ll 1$ is valid, ω_* must satisfy the following relation.

$$\omega_* \geq \frac{K_*(1-A_*)-K_0(1-A_0)}{\theta_*-\theta_0} \qquad \text{for} \quad \theta_* \leq \theta_c' \tag{93}_1$$

$$\omega_* \geq \frac{K_c'(1-A_c')-K_0(1-A_0)}{\theta_c'-\theta_0} \qquad \text{for} \quad \theta_* > \theta_c' \tag{93}_2$$

where the subscript $'_c$ means the value at $\theta=\theta_c'$. However, from Eq. (89), θ_* must satisfy the following condition.

$$\theta_* \leq \theta_c' \tag{94}$$

Therefore, the condition of existence of ω_* is given by Eq. $(93)_1$.

(2) Profile of wetting front

From Eq. (88) and Eq. (90), we get the following equation.

$$\frac{d\zeta}{d\theta} = \frac{D(1-A)}{\dfrac{\theta-\theta_0}{\theta_*-\theta_0}\{K_*(1-A_*)(1-\eta_*)-K_0(1-A_0)\}-K(1-A)+KA\left(\dfrac{K_a}{K}\eta\right)+K_0(1-A_0)} \tag{95}$$

Integrating this equation with respect to θ yields

$$\zeta-\zeta_*^{\Delta}=-\int_{\theta}^{\theta_*-\Delta_*}\frac{D(1-A)}{-\dfrac{\theta-\theta_0}{\theta_*-\theta_0}\{K_*(1-A_*)(1-\eta_*)-K_0(1-A_0)\}+K(1-A)-KA\left(\dfrac{K_a}{K}\eta\right)-K_0(1-A_0)}d\theta \tag{96}$$

where ζ_*^{Δ} is the value at $\theta=\theta_*-\Delta_*$ and Δ_* is a certain small positive value. Especially, in case of $|\eta|\ll 1$, it becomes

$$\zeta-\zeta_*^{\Delta}=-\int_{\theta}^{\theta_*-\Delta_*}\frac{D(1-A)}{-\dfrac{\theta-\theta_0}{\theta_*-\theta_0}\{K_*(1-A_*)-K_0(1-A_0)\}+K(1-A)-K_0(1-A_0)}d\theta \tag{97}$$

If Δ_* is given, the moisture profile of the wetting front can be calculated numerically by Eq. (97).

(3) Rate of change of pore-air pressure with time

From Eq. (81) and Eq. (87), the following equation is obtained.

$$\frac{\partial p_a}{\partial\zeta}=\frac{1}{K}\left\{K-(\theta-\theta_0)\omega_*-D\frac{d\theta}{d\zeta}+K_0(1-A_0)\right\} \tag{98}$$

As the right side of this equation is the function of θ or ζ, it is known that p_a is represented by the sum of a function of ζ and a function of τ. And as v_a between the lower end of the wetting front and the bottom of layer can be considered nearly zero, it results from Eq. (7) and Eq. (34) that $\partial p_a/\partial x\approx 0$. As from these results, the pore-air pressure p_a at $\theta\to\theta_{0+}$ in the wetting front is considered to be nearly equal to that at the bottom of layer, p_{aL}, we get

$$\frac{\partial p_a}{\partial\tau}\approx\frac{dp_{aL}}{dt} \tag{99}$$

And, from Eq. (80), $\partial p_a/\partial\tau$ is given by,

$$\frac{\partial p_a}{\partial\tau}=\omega_*\left(\frac{\partial p_a}{\partial\zeta}\right)_*+u(\tau) \tag{100}$$

$(\partial p_a/\partial\zeta)_*$ in the above equation is given by Eq. (82) and Eq. (87) as follows:

$$\left(\frac{\partial p_a}{\partial\zeta}\right)_*=1-\frac{\omega_*(\theta-\theta_0)}{K_*}-\frac{K_0(1-A_0)}{K_*} \tag{101}$$

Furthermore, introducing Eq. (88) into ω_* in the above equation, we get

$$\left(\frac{\partial p_a}{\partial\zeta}\right)_*=A_*+(1-A_*)\eta_* \tag{102}$$

Especially in case of $|\eta_*| \ll 1$, Eq. (102) becomes

$$\left(\frac{\partial p_a}{\partial \zeta}\right)_* = A_* \tag{103}$$

Finally, applying Eq. (101) or Eq. (102) to Eq. (100), the following equations are obtained.

$$\frac{\partial p_a}{\partial \tau} = \omega_* \left\{1 - \frac{\omega_*(\theta-\theta_0)}{K_*} - \frac{K_0(1-A_0)}{K_*}\right\} + u(\tau) \tag{104}$$

$$\frac{\partial p_a}{\partial \tau} = \frac{K_*(1-A_*)(1-\eta_*) - K_0(1-A_0)}{\theta_*-\theta_0} \{A_* + (1-A_*)\eta_*\} + u(\tau) \tag{105}$$

(4) Profile of pore-air pressure

After multiplying Eq. (84) by $d\zeta/d\theta$ given by Eq. (95), integrating with respect to θ, and using Eq. (79), Eq. (87), the following equation is obtained.

$$p_a - (p_a)_*^A = \int_\theta^{\theta_*-A_*} \frac{AD}{K} d\theta - \int_\theta^{\theta_*-A_*} \frac{AD(1-A)\left(1+\dfrac{K_a}{K}\eta\right)}{-\dfrac{\theta-\theta_0}{\theta_*-\theta_0}\{K_*(1-A_*)(1-\eta_*) - K_0(1-A_0)\} + K(1-A) - K_0(1-A_0) - AK\left(\dfrac{K_a}{K}\eta\right)} d\theta \tag{106}$$

where $(p_a)_*^A$ is the value of p_a at $\zeta=\zeta_*^A$. Especially in case of $|\eta| \ll 1$, Eq. (106) becomes

$$p_a - (p_a)_*^A = \int_\theta^{\theta_*-A_*} \frac{AD}{K} d\theta - \int_\theta^{\theta_*-A_*} \frac{AD(1-A)}{-\dfrac{\theta-\theta_0}{\theta_*-\theta_0}\{K_*(1-A_*) - K_0(1-A_0)\} + K(1-A) - K_0(1-A_0)} d\theta \tag{107}$$

(5) Examination of induced relations

(a) validity of assumption $|\eta_*| \ll 1$

Let us examine the validity the equations induced in (1)~(4) by using the observed values. The values of v_0 and v_{a_0} given by Eq. (78) and Eq. (79), respectively, can be set to be zero, because of the initial condition Eq. (28), and the boundary conditions Eq. (30) and Eq. (31) in the experiment. It results that $\theta_0 \to 0$, $K_0 \to 0$ for $v_0 \to 0$ and that $(\partial p_a/\partial\zeta)_0 \to 0$, $A_0 \to 0$ for $v_{a_0} \to 0$.

Firstly, let us examine the order of $(\partial p_a/\partial\zeta)_*$. As the wetting front advances downwards, ω_* is positive. From Eq. (82) and $\omega_* > 0$, the following relation is obtained.

$$1 > \left(\frac{\partial p_a}{\partial \zeta}\right)_* > 0 \tag{108}$$

As $(\partial p_a/\partial\zeta)_*$ is expressed by A_* and η_* in Eq. (102), let us examine the values of A_* and η_*. In case of Sand K-7, for example, using 0.36~0.38 as θ_* by referring to **Table 2** and 1.8~2, given in **6.1**, as the parameter A in Eq. (71) which expresses the permeability of pore-air $K_a(\theta)$, the value of A_* is 0.1~0.14 for $A=1.8$ and 0.18~0.27 for $A=2$. Next, η_* can be expressed by the order estimation as follows:

$$\eta_* \sim -\frac{\theta_s}{K_{a*}P_{a_0}}\dot{p}_{a\infty}L \tag{109}$$

Then, the ratio of two terms in the right hand side of Eq. (102) becomes

$$\frac{(1-A_*)|\eta_*|}{A_*} \sim \frac{\theta_s L}{K_* P_{a_0}}\dot{p}_{a\infty} \tag{110}$$

Calculating the value of the right hand side of the above equation under such a condition that $\theta_*=0.37$, $K_*=4\times10^{-3}$ or 1×10^{-2} cm/sec, $\dot{p}_{a\infty}=2\times10^{-3}$ or 1×10^{-2} cmAq/sec for Sand K-7 or Sand K-6 by referring to **Table 2**, we get 4×10^{-2} for Sand K-7 and 7×10^{-2} for Sand K-6, where $\theta_s=0.46$, $P_{a_0}=10^3$ cmAq and $L=160$ cm. As this means that $(1-A_*)|\eta_*|/A_* \ll 1$, that is, $A_*+(1-A_*)\eta_* \approx A_*$ or $|\eta_*| \ll 1$, the validity of Eq. (103) and also the validity of Eq. (89), Eq. (92), Eq. (97) and Eq. (107) are confirmed.

(b) estimation of several characteristic quantities

The value of ω_*: Let us pay attention to ω_* given by Eq. (89). As K_0, A_0 and θ_0 are equal to zero and A_* is small in comparison with 1, in this case $\omega_* \approx K_*/\theta_*$. Actually comparing ω_* with K_*/θ_* shown in **Table 2**, it is found out that ω_* is about equal to K_*/θ_*.

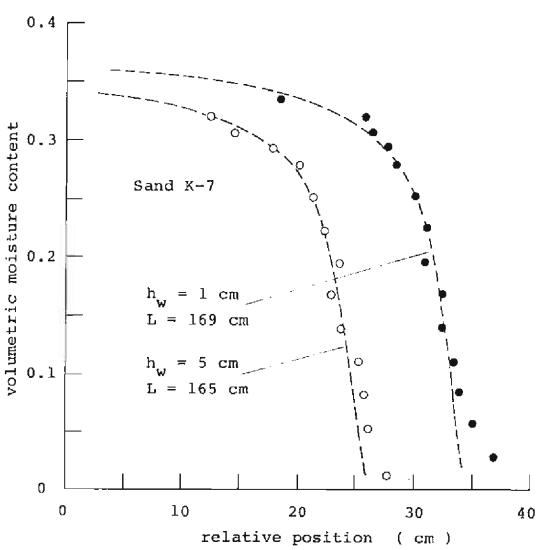

Fig. 17. Comparison between calculated moisture profile of wetting front and observed ones, in the case of Sand K-7.

The profile of wetting front: Using Eq. (97) under the same assumption as above, we can get the profile of wetting front by giving the value of θ_* and the small value of Δ_*. **Fig. 17** is the comparison of the calculated profile with the observed one, corresponding to **Fig. 2** (**a**), which is given by finding out the value of intersection of the x-axis and the broken line, for example, shown in **Fig. 14** (**a**). Two examples of calculation, $\theta_*=0.37$ in case of $h_w=1$ cm and $\theta_*=0.36$ in case of $h_w=5$ cm show a good agreement with the observed ones.

The value of $u(\tau)$: Considering Eq. (99), $(\partial p_a/\partial\tau)_*$ in Eq. (80) remains constant, because of the observed fact that $dp_{aL}/dt=$constant. Then, applying $(\partial p_a/\partial\tau)_*=$ constant and $(\partial p_a/\partial\zeta)_*=$constant to Eq. (80), $u(\tau)$ is to be constant because of the observed fact that $\omega_*=$constant. We represent this as u_0.

5. Solutions of fundamental equations[18),19),21)]

5.1 Solution for quasi-saturated zone with parameters defined at the boundary of its lower end

The fundamental equations for the quasi-saturated zone are given by Eq. (24) and Eq. (27), in which the pore-air pressure at the lower end of the zone, p_{a_1}, and the filter velocity throughout the zone, $\hat{v}$, can be calculated easily if the value of α_r, β_r, ψ_1, p_{w_0}, x_1, and $\hat{K}$ are given.

Let us first pay attention to Eq. (23) or Eq. (24) and Eq. (27). As the velocity of water is relatively slow, p_{w_0} can be given by,

$$p_{w_0} \approx h_w \tag{111}$$

The movement of air throughout the quasi-saturated zone is hardly inspectable by the naked eye. In order to imagine this process, the supplemental experiment in which the U-shaped tube is used, was carried out as described in **Appendix**. Owing to the results obtained by the experiment, it is known that the formation of an air bubble and its separation from the air in the U-shaped tube are in correspondence with the invasion of the pore-air in the unsaturated zone into the quasi-saturated zone and the escape of the pore-air from the sand surface, respectively. So, p_{a_0} can be given approximately as

$$p_{a_0} \approx h_w \tag{112}$$

In order to find the physical expression of $(1-\alpha_r)\psi_1$, in Eq. (23), assuming that Eq. (23) is valid also at $h_w\approx 0$, $x_1\approx 0$, and considering Eq. (111), Eq. (112) and the result shown in **Appendix**, the following relation can be given.

$$(1-\alpha_r)\psi_1 \rightarrow \psi_e \tag{113}$$

where ψ_e corresponds to the water or air entry value of the U-shaped tube. The sign $\rightarrow$ means that the term $(1-\alpha_r)\psi_1$ becomes ψ_e after some time goes by.

From Eq. (111) and Eq. (112), the three relations of Eq. (27), Eq. (24) and Eq. (26) become:

$$f = \alpha_r \hat{K}\left(1-\frac{\psi_1}{x_1}\right) \tag{114}$$

$$p_{a_1}-h_w = (1-\alpha_r)\,(x_1-\psi_1) \quad \cdots\cdots(115) \qquad \beta_r = -\alpha_r\psi_1\,, \tag{116}$$

respectively. In the early stage of infiltration it is known that the infiltration rate, the pore-air pressure, p_{aL}, at the bottom of layer and the movement of moisture obey Eq. (2), Eq. (1) and Eq. (4), respectively. And as p_{a_1} changes approximately in a similar manner to p_{aL}, we get the following equation:

$$p_{a_1}-h_w = a \ln t + b' \tag{117}$$

where b' is a certain constant. So, from Eq. (114) and Eq. (2), and from Eq. (115) and Eq. (117) we can get, respectively,

$$\alpha_r = \frac{S\varphi_1}{2}\Big/\left\{\frac{S\varphi_1}{2}+\hat{K}(a \ln t+b')\right\} \tag{118}$$

$$\psi_1 = t^{1/2}\varphi_1-\left\{\frac{S\varphi_1}{2}+\hat{K}(a \ln t+b')\right\}\Big/\hat{K} \tag{119}$$

where φ_1 is $\varphi(\theta_1, t)$. And applying these equations to Eq. (116), we obtain finally,

$$\beta_r = \frac{S\varphi_1}{2}\Big/\hat{K}-\frac{S\varphi_1}{2}\,\varphi_1 t^{1/2}\Big/\left\{\frac{S\varphi_1}{2}+\hat{K}(a \ln t+b')\right\} \tag{120}$$

Let us examine the characteristics of α_r, β_r and ψ_1 by using the experimental results of Sand K-7 and Sand K-6 in $h_w=1$ cm, $L=169$ cm, shown before in **Fig. 7** (**a**) and **Fig. 8**, respectively. Though the values of S, a and b are shown in **Table 1**, the values of b' and φ_1 cannot be estimated. So, let us apply the approximation $b=b'$ and the value $\varphi_1=0.2$, 0.4 cm/sec$^{1/2}$ estimated roughly for each case to Eqs. (117), (118), (119) and (120). The calculated results are shown in **Fig. 18** (**a**) and (**b**) for Sand K-7 and in **Fig. 19** (**a**) and (**b**) for Sand K-6, where $\hat{K}$ is considered to be constant and the values of $\hat{K}$ mentioned in **6.1** are used. It is found out from these figures that α_r decreases abruptly just after the beginning of infiltration and decreases slowly as time goes by, and that β_r decreases very slowly as time goes by, and further that $-\psi_1$ increases abruptly just after the beginning and then changes moderately. These properties are recognized in the other cases.

As the infiltration rate, the pore-air pressure and the moving velocity of the wetting front become constant approximately after a long time has elapsed, α_r defined by Eq. (25) is also expected to become constant α_c. Combining this characteristics of α_r and Eq. (113), it is seen that β_r also approaches a constant value, β_c, asymptotically.

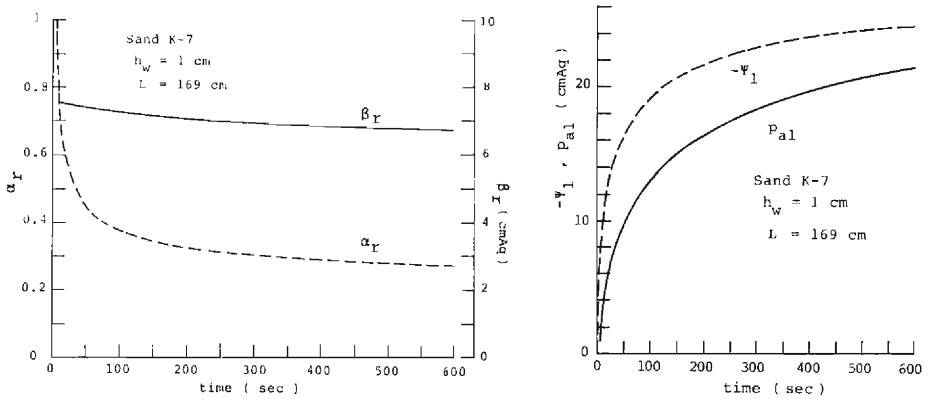

(a) (b)

Fig. 18. Changes of α_r, β_r and $-\psi_1$, p_{a1} with time in the case of Sand K-7.
(a) α_r, β_r
(b) $-\psi_1$, p_{a1}

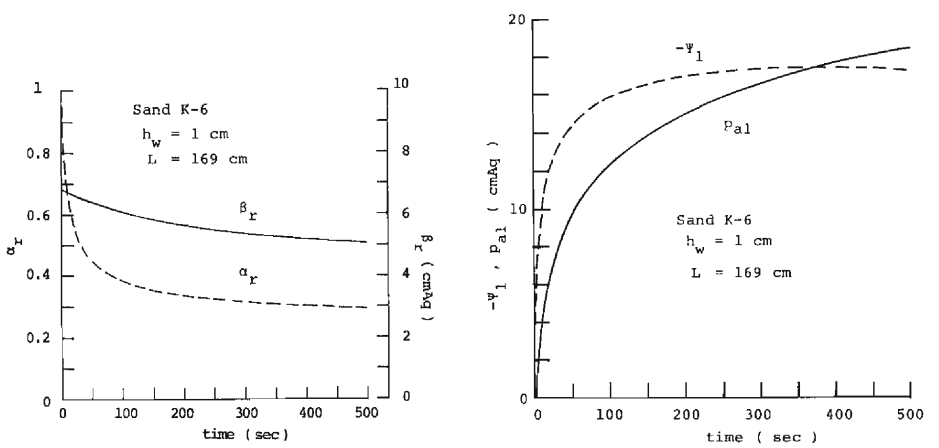

(a) (b)

Fig. 19. Same as Fig. 18, but in the case of Sand K-6.
(a) α_r, β_r
(b) $-\psi_1$, p_{a1}

$$\alpha_r \to \alpha_c \qquad (121) \qquad \beta_r \to \beta_c \qquad (122)$$

Under the extreme condition, ψ_1 and β_c are given, respectively, by,

$$\psi_1 \to \frac{\psi_e}{1-\alpha_c} \qquad (123) \qquad \beta_c = -\frac{\alpha_c}{1-\alpha_c}\psi_e \qquad (124)$$

It is possible to know the parameters included in the fundamental relations Eqs. (114), (115) and (116), excluding the parameter x_1 or $\hat{v}$ and p_{a1} at the lower boundary of the quasi-saturated zone, as mentioned above. Therefore, these rela-

tions can be considered as the solution with a parameter x_1 or $\hat{v}$ and p_{a1} for the quasi-saturated zone.

5.2 Solution for unsaturated zone with parameters defined at the boundary of its upper end

The fundamental equations are given by Eq. (14) for the water, and Eqs. (15) and (16) for the pore-air in the unsaturated zone beneath the quasi-saturated zone and the initial conditions Eqs. (28) and (29). The boundary conditions are given by Eqs. (19), (20) at $x=L$ and the following ones at $x=x_1$.

$$\theta = \theta_1 \qquad (125) \qquad v = \hat{v} = f \qquad (126)$$

$$v_a = \hat{v}_a \qquad (127)$$

where θ_1 is water content at the boundary $x=x_1$.

In order to find out approximate solutions, let us assume that

$$|\Delta p_a(x, t)| / \bar{P}_a(t) \ll 1 \qquad (128)$$

where
$$P_a(x, t) = \bar{P}_a(t) + \Delta p_a(x, t) \qquad (129)$$

that is, the pore-air pressure is expressed by the sum of the average pressure in the unsaturated zone, $\bar{P}_a(t)$, and the deviation from it, $\Delta p_a(x, t)$. Then the following relation can be obtained from Eqs. (14), (15), (16), (30) and (31),

$$\frac{\partial p_a}{\partial x} = -\frac{AD}{K}\frac{\partial \theta}{\partial t} + A(1-\varepsilon) + (1-A)\frac{\rho_a}{\rho_w} \qquad (130)$$

where A is defined by Eq. (59) and

$$\varepsilon = \int_x^L (\theta_s - \theta)\frac{\partial P_a}{\partial t}\, dx / K\bar{P}_a \qquad (131)$$

Eq. (14) and Eq. (130) become the approximate fundamental equations in the domain under consideration.

Using θ and t instead of x and t as the independent variables, these equations can be described as follows:

$$-\frac{\partial x}{\partial t} = \frac{\partial}{\partial \theta}\left[D \Big/ \frac{\partial x}{\partial \theta} - K\left\{1 - \left(\frac{\partial p_a}{\partial \theta} \Big/ \frac{\partial x}{\partial \theta}\right)\right\}\right] \qquad (132)$$

$$\frac{\partial p_a}{\partial \theta} \Big/ \frac{\partial x}{\partial \theta} = -\frac{DA}{K} \Big/ \frac{\partial x}{\partial \theta} + A(1-\varepsilon) + (1-A)\frac{\rho_a}{\rho_w}, \qquad (133)$$

respectively.

(1) First approximation

Putting $\partial x/\partial t = 0$ in Eq. (132) following Parlange's method,[22] and integrating with respect to θ, we get,

$$\frac{\partial x}{\partial \theta} = \frac{D}{-f+K\left\{1-\left(\frac{\partial p_a}{\partial \theta}\Big/\frac{\partial x}{\partial \theta}\right)\right\}} \tag{134}$$

After introducing Eq. (133) into Eq. (134), integrating with respect to θ, the following relation is obtained.

$$x = x_1 - \int_{\theta}^{\theta_1} \frac{D(1-A)}{-f+K(1-A)\left(1-\frac{\rho_a}{\rho_w}\right)+KA\varepsilon}\, d\theta \tag{135}$$

Let us consider the approximate expression for the denominator of the integrand in the above equation. First, we can put $1-(\rho_a/\rho_w)\approx 1$ because of $\rho_a/\rho_w \approx 10^{-3}$. Next, we obtain $KA\varepsilon \sim (\theta_s AL/\bar{P}_a)dp_{aL}/dt$, by applying the order estimation to the equation of the definition of ε, Eq. (131). Applying $\theta_s \approx 0.46$, $\bar{P}_a \approx 10^3$ cmAq and $L \approx 10^2$ cm in our experiments to this relation, it is seen that $KA\varepsilon \sim 5\times 10^{-2} A dp_{aL}/dt$. In the stage where the quasi-saturated zone develops enough, it is shown in **Table 2** that the infiltration rate becomes larger than 3×10^{-3} cm/sec for Sand K-7 and 1×10^{-2} cm/sec for Sand K-6 and that the rate of change of pore-air pressure is roughly in the order of 10^{-3} cmAq/sec for Sand K-7 and 10^{-2} cmAq/sec for Sand K-6. Then, $AK\varepsilon/f \sim 1.7\times 10^{-2}$ for Sand K-7 and 5×10^{-2} for Sand K-6. Therefore as $A<1$ from the definition of A, Eq. (59), we get the following relation.

$$KA\varepsilon \ll f \tag{136}$$

Then, Eq. (135) can be approximated as

$$x = x_1 - \int_{\theta}^{\theta_1} \frac{D(1-A)}{-f+K(1-A)}\, d\theta \tag{137}$$

Moreover, the mass conservation of water under the condition Eq. (126) must be satisfied as follows:

$$f = \int_0^{\theta_1} \frac{\partial x}{\partial t}\, d\theta = \theta_1 \frac{dx_1}{dt} - \int_0^{\theta_1} \theta W\, d\theta \tag{138}$$

where
$$W = \frac{D(1-A)}{\{-f+K(1-A)\}^2} \tag{139}$$

And x_1 is given by Eq. (27) as follows:

$$x_1 = \frac{\beta_r \hat{K}}{f-\alpha_r \hat{K}} \tag{140}$$

From Eq. (140), dx_1/dt is given by

$$\frac{dx_1}{dt} = -Z\frac{df}{dt} + R \tag{141}$$

where $$Z(t)=\frac{\beta_r\hat{K}}{(f-\alpha_r\hat{K})^2},\quad R(t)=\hat{K}\frac{(f-\alpha_r\hat{K})\frac{d\beta_r}{dt}+\beta_r\hat{K}\frac{d\alpha_r}{dt}}{(f-\alpha_r\hat{K})^2} \tag{142}$$

Introducing Eq. (141) into Eq. (138), we get,

$$\frac{df}{dt}=-\frac{f-\theta_1 R}{\int_0^{\theta_1}\theta W d\theta+\theta_1 Z} \tag{143}$$

and, inserting Eq. (143) into Eq. (141), we can obtain

$$\frac{dx_1}{dt}=\frac{R\int_0^{\theta_1}d\theta\int_\theta^{\theta_1}Wd\theta+fZ}{\int_0^{\theta_1}d\theta\int_\theta^{\theta_1}Wd\theta+\theta_1 Z}\equiv\left(\frac{dx_1}{dt}\right)_0 \tag{144}$$

Eqs. (137) and (143) are the first approximation of the solution for the unsaturated zone.

(2) Second approximation

Differentiating Eq. (137) partially with respect to t, and using Eq. (143) and Eq. (144), we get,

$$\frac{\partial x}{\partial t}=R+\frac{\int_0^{\theta_1}Wd\theta+Z}{\int_0^{\theta_1}\theta Wd\theta+\theta_1 Z}(f-\theta_1 R) \tag{145}$$

After assuming that $\partial x/\partial t$ given by Eq. (145) is equal to $\partial x/\partial t$ given by Eq. (132), following Parlange's method,[22] integrating it with respect to θ while considering Eqs. (28) and (30), and introducing Eq. (133) into the result obtained, we get,

$$\frac{\partial x}{\partial\theta}=\frac{D(1-A)}{K(1-A)\left(1-\frac{\rho_a}{\rho_w}\right)+KA\varepsilon-\theta\left(\frac{dx_1}{dt}\right)_0-\left\{f-\theta_1\left(\frac{dx_1}{dt}\right)_0\right\}I} \tag{146}$$

where

$$I=\frac{\int_0^{\theta}d\theta\int_\theta^{\theta_1}Wd\theta}{\int_0^{\theta_1}d\theta\int_\theta^{\theta_1}Wd\theta} \tag{147}$$

Let us consider the approximation of the denominator of the right hand side of Eq. (146). As mentioned before, $1-(\rho_a/\rho_w)\approx 1$. And the estimation of ε term is as follows. For the large value of θ, we may state that $\varepsilon=0$, because the condition Eq. (136) is satisfied. For the small value of θ, we can neglect $KA\varepsilon$ compared with $K(1-A)$. Then, putting $\varepsilon=0$ approximately, integrating with respect to θ and using Eq. (125), Eq. (146) becomes:

$$x = x_1 - \int_{\theta}^{\theta_1} \frac{D(1-A)}{K(1-A) - \theta\left(\frac{dx_1}{dt}\right)_0 - \left\{f - \theta_1\left(\frac{dx_1}{dt}\right)_0\right\} I} d\theta \tag{148}$$

where x_1 is given by Eq. (140). Eq. (148) must satisfy the following equation on the mass conservation of water[23].

$$\int_0^t f\,dt = \int_0^{\theta_1} x\,d\theta = \theta_1 x_1 - \int_0^{\theta_1} \frac{\theta D(1-A)}{K(1-A) - \theta\left(\frac{dx_1}{dt}\right)_0 - \left\{f - \theta_1\left(\frac{dx_1}{dt}\right)_0\right\} I} d\theta \tag{149}$$

Eq. (148) and Eq. (149) give the second approximation of solution of the water movement.

Next, multiplying Eq. (133) by $\partial x/\partial\theta$ given in Eq. (146), applying the assumption $1-(\rho_a/\rho_w)\approx 1$ and integrating with respect to θ the result obtained, we get,

$$p_a(\theta, t) = p_a(\theta_1, t) + \int_{\theta}^{\theta_1} \frac{AD}{K} d\theta - \int_{\theta}^{\theta_1} \frac{AD(1-A)(1-\varepsilon)}{K(1-A) + KA\varepsilon - \theta\left(\frac{dx_1}{dt}\right)_0 - \left\{f - \theta_1\left(\frac{dx_1}{dt}\right)_0\right\} I} d\theta \tag{150}$$

where $p_a(\theta_1, t)$ is equal to p_{a1} given in Eq. (115). And putting $\varepsilon=0$ in Eq. (150) for the same reason as Eq. (148), we get,

$$p_a(\theta, t) = p_a(\theta_1, t) + \int_{\theta}^{\theta_1} \frac{AD}{K} d\theta - \int_{\theta}^{\theta_1} \frac{AD(1-A)}{K(1-A) - \theta\left(\frac{dx_1}{dt}\right)_0 - \left\{f - \theta_1\left(\frac{dx_1}{dt}\right)_0\right\} I} d\theta \tag{151}$$

The pore-air pressure at the bottom of layer can be given approximately by putting $\theta \to 0_+$ in Eq. (151).

The condition of mass conservation of air given by Eq. (127) is not yet applied. After transforming Eq. (10) and Eq. (7), giving v and v_a, respectively, by using θ, t as the independent variables, finding the sum of these equation under consideration of Eq. (146) and Eq. (150), we obtain,

$$V_t(\theta, t) \equiv v + v_a = K\varepsilon \tag{152}$$

where $1-(\rho_a/\rho_w)\approx 1$. Considering Eq. (126) and Eq. (127), this condition at $\theta=\theta_1$ becomes:

$$V_t(\theta_1, t) = \hat{v} + \hat{v}_a = K(\theta_1)[\varepsilon]_{x=x_1+} \tag{153}$$

As we are considering the case of $\varepsilon=0$, $(\hat{v}+\hat{v}_a)$ becomes zero. From this, $r(t)$ defined in Eq. (22) becomes

$$r(t) = 1 \tag{154}$$

Let us denote α_r and β_r for this case, $r=1$, especially as follows:

$$\alpha_r \to \alpha\,, \quad \beta_r \to \beta \tag{155}$$

Finally, the second approximations with the parameters x_1 and p_{a1} for the unsaturated zone are given by Eq. (148), Eq. (149) and Eq. (151) under the condition of Eq. (155).

(3) Accuracy of approximate solution

In order to examine the accuracy of the second approximate solution for the unsaturated zone, let us compare it with the results obtained directly from Eq. (14) and Eq. (130), with $\varepsilon=0$ and $\rho_a/\rho_w=0$, under convenient conditions which will be explained later.

(a) several characteristics obtained from Eqs. (14) and (130) under the condition $\varepsilon=0$ and $\rho_a/\rho_w=0$

Introducing Eq. (130), putting $\varepsilon=0$ and $\rho_a/\rho_w=0$, into Eq. (14), we get

$$\frac{\partial\theta}{\partial t}=\frac{\partial}{\partial x}\left\{D(1-A)\frac{\partial\theta}{\partial x}-K(1-A)\right\} \tag{156}$$

From this equation, the filter velocity of water is given by

$$v=-D(1-A)\frac{\partial\theta}{\partial x}+K(1-A) \tag{157}$$

It is already known from **2.2** (2) that after a long time has elapsed, both the velocity of the wetting front and the rate of infiltration approach a constant value. Here, although the sand layer in the experiment is not so thick, it is assumed that its thickness is large enough to determine the characteristics of infiltration phenomenon in the so-called critical state.

i) infiltration rate

As it is expected that $\partial\theta/\partial x\leq 0$ and $A<1$ during the supplying of water, the following relation is satisfied from Eq. (157),

$$f\geq K(1-A) \tag{158}_1$$

For example, the shape of function $K(1-A)$ is already shown in **Fig. 16** for Sand K-7. The function $K(1-A)$ has the largest value at a moisture content θ_c. Then, Eq. $(158)_1$ is to be rewritten as follows:

$$f\geq\{K(1-A)\}_c \tag{158}_2$$

where the subscript c means the value at $\theta=\theta_c$.

The experimental results show that, after a long time has elapsed, the infiltration rate approaches a constant value, f_∞, and that the development of the quasi-saturated zone almost stops and the depth of the zone is relatively shallow, as mentioned in **6.1**. As the moisture content at a finite depth of the unsaturated zone

remains almost unchangeable with time, the value of v should become equal f_∞ at such depth. Moreover, as the wetting front must be advancing to a very deep position, there appears $\partial\theta/\partial x \approx 0$ at a certain moisture content, $\theta_n (<\theta_1)$. Therefore, by considering that v at $\theta=\theta_n$ is $\{K(1-A)\}_{\theta_n}$, it is known that $\theta_n=\theta_c$ and

$$f_\infty = \{K(1-A)\}_c \tag{159}$$

ii) moisture profile

From Eq. (157), the moisture profile in $\theta_1 \geq \theta > \theta_c$ is given as:

$$x = x_1 - \int_\theta^{\theta_1} \frac{D(1-A)}{K(1-A)-f_\infty} d\theta \tag{160}$$

In **4.2** it is described that the nearly constant moisture content θ_* in the transmission zone satisfies Eq. (94) and that the velocity of wetting front is given by Eq. (89), in the case of $|\eta_*| \ll 1$. It is obvious that $\varepsilon \approx 0$ corresponds to $|\eta| \approx 0$ because of the equations of definition for ε and η, *i.e.* Eq. (131) and Eq. (85). As mentioned in **Fig. 16**, θ_c is slightly larger than θ_c' but nearly equal to θ_c', in which θ_c' is defined in **Fig. 16**. For example, in the case of Sand K-7, $\theta_c \approx 0.38$ and $\theta_c' \approx 0.36$. Considering that the wetting front is advancing with a constant velocity and has a constant profile, the filter velocity of water v_* at $\theta=\theta_*$ is given by:

$$v_* \approx K_*(1-A_*) \tag{161}$$

because $1/(\partial x/\partial\theta)=0$ at $\theta=\theta_*$. **Fig. 20** shows a schematic profile of moisture content under consideration. As v at $\theta=\theta_{c+}$ and $\theta=\theta_{*-}$ are given by Eq. (159) and Eq. (161), respectively, v_{c+} becomes larger than v_{*-}. And as the functions, $K(1-A)$ and $D(1-A)$, are considered to be smooth with θ and $\partial\theta/\partial x$ becomes almost zero at $\theta \to \theta_c$ and $\theta \to \theta_*$, the following relations are obtained at $\theta=\theta_c-\Delta_1$ and $\theta=\theta_*+\Delta_2$

$$K(1-A) \gg -D(1-A)\frac{\partial\theta}{\partial x} \tag{162}$$

$$v \approx K(1-A) \tag{163}$$

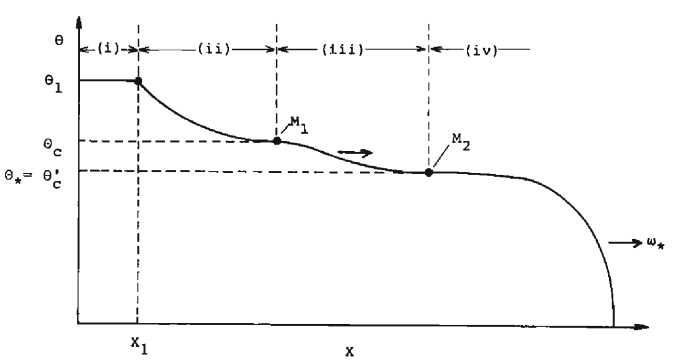

Fig. 20. Schematic moisture profile in the critical state.

because $\partial\theta/\partial x \approx 0$ at these points, where Δ_1 and Δ_2 are positive and small quantities. Applying Eq. (163) to Eq. (156), we get,

$$\frac{\partial\theta}{\partial t}+\frac{d}{d\theta}K(1-A)\cdot\frac{\partial\theta}{\partial x}=0 \tag{164}$$

As this equation has such a solution as θ=constant on the characteristic curve of $dx/dt=dK(1-A)/d\theta$, dx/dt becomes $\{dK(1-A)/d\theta\}_c$ at $\theta=\theta_c-\Delta_1$ and $\{dK(1-A)/d\theta\}_*$ at $\theta=\theta_*+\Delta_2$, for Δ_1, $\Delta_2\to 0$. Owing to the definition of θ_c, $\{dK(1-A)/d\theta\}_c$ is equal to zero. Considering the physical condition that $\{dK(1-A)/d\theta\}_*$ must coincide with the velocity of the wetting front $\omega_*=\{K(1-A)\}_*/\theta_*$, θ_* is given as follows:

$$\theta_*=\theta_c' \tag{165}$$

And as $\theta_*=0.36\sim 0.38$ for Sand K-7 in **Table 2**, it is obvious that θ_* is nearly equal to $\theta_c'\approx 0.36$.

The propagating velocity $\partial x/\partial t$ of the intermediate moisture content between $\theta=\theta_{c_-}$ and $\theta=\theta_{c_+}'$ is not exactly clear. But as there is such a relation as $\theta_c\approx\theta_c'$, and the distance from the point M_1 to the point M_2 in **Fig. 20** is considered to be far to some extent, Eq. (162) is satisfied with such moisture contents. Therefore, the following relation remains valid for $\theta_{c_-}>\theta>\theta_{c_+}'$

$$\theta=\text{constant} \qquad \text{on} \quad \frac{dx}{dt}=\frac{dK(1-A)}{d\theta} \tag{166}$$

It is known from this that the domain of $\theta_{c_-}>\theta>\theta_{c_+}'$ is stretched out as time proceeds, because $d^2K(1-A)/d\theta^2<0$. And it is obvious that Eq. (166) satisfies the following mass conservation equation for the domain between $\theta=\theta_c$ and $\theta=\theta_c'(=\theta_*)$.

$$v_c-v_c'=\{K(1-A)\}_c-\{K(1-A)\}_c'=\int_{\theta_c'}^{\theta_c}\frac{\partial x}{\partial t}d\theta \tag{167}$$

In summary, referring to **Fig. 20**, the moisture profile is composed of, in the gravitational direction, (i) the quasi-saturated zone of $\theta=\theta_1$, (ii) the zone of $\theta_1>\theta>\theta_c$ where the moisture profile is almost unchangeable and is given by Eq. (160), and where $\partial\theta/\partial x$ becomes zero at $\theta=\theta_{c_+}$, (iii) the stretching zone of $\theta_c>\theta>\theta_c'$ where the moisture with a constant content moves on mathematical characteristic curves, its velocity being zero at θ_{c_-} and $\{K(1-A)/\theta\}_c'$ at $\theta=\theta_{c_+}'$, where $\partial\theta/\partial x$ at $\theta=\theta_c$ and $\theta=\theta_c'$ become zero, and (iv) the transmission zone of $\theta=\theta_c'$ and the wetting front ahead of it with the constant velocity $\{K(1-A)/\theta\}_c'$ and an unchangeable profile. All zones of (ii), (iii) and (iv) together are called the unsaturated zone.

(b) examination of the accuracy of the second approximation

After a long time has elapsed, the following relations can be determined from Eqs. (148), (149) and (151).

infiltration rate;

$$f'_\infty = \frac{\theta_c}{\theta'_*} K'_*(1-A'_*) \tag{168}$$

profile of moisture content;

$$x = x_1 - \int_\theta^{\theta_1} \frac{D(1-A)}{K(1-A)-f'_\infty} d\theta \qquad \text{for} \quad \theta > \theta_c \tag{169}_1$$

$$x = x_1 - \int_\theta^{\theta_1} \frac{D(1-A)}{K(1-A)-\dfrac{\theta}{\theta_c} f'_\infty} d\theta \qquad \text{for} \quad \theta < \theta_c \tag{169}_2$$

celerity of moisture content;

$$\frac{\partial x}{\partial t} \approx 0 \qquad \text{for} \quad \theta > \theta_c \tag{170}_1$$

$$\frac{\partial x}{\partial t} \approx \frac{2\theta_c}{\theta'_* + \theta_c} \frac{K'_*(1-A'_*)}{\theta'_*} \qquad \text{for} \quad \theta < \theta_c \tag{170}_2$$

profile of pore-air pressure;

$$p_a(\theta, t) - p_a(\theta'_* - \Delta'_*, t) = \int_\theta^{\theta'_* - \Delta'_*} \frac{AD}{K} d\theta - \int_\theta^{\theta'_* - \Delta'_*} \frac{AD(1-A)}{K(1-A) - \dfrac{\theta}{\theta'_*} K'_*(1-A'_*)} d\theta$$

$$\text{for} \quad \theta < \theta'_* - \Delta'_* \tag{171}$$

change of pore-air pressure with time;

$$\frac{\partial}{\partial t}\{p_a(\theta, t) - p_a(\theta_1, t)\} \approx 0 \qquad \text{for} \quad \theta > \theta_c \tag{172}_1$$

$$\frac{\partial}{\partial t}\{p_a(\theta, t) - p_a(\theta_1, t)\} \approx \frac{K'_*(1-A'_*)}{\theta'_*} A'_* \qquad \text{for} \quad \theta < \theta_c \tag{172}_2$$

where θ'_* satisfies the condition that

$$K'_*(1-A'_*) - \theta'_* \left(\frac{dx_1}{dt}\right)_0 - \left\{f'_\infty - \theta_1 \left(\frac{dx_1}{dt}\right)_0\right\} I'_* \approx 0 \tag{173}$$

The affix $'_*$ means that the value at $\theta = \theta'_*$ and Δ'_* is a positive and small quantity. Eq. (168) to Eq. (173) have been induced from the condition that the quasi-saturated zone does not develop infinitely and, especially, in Eq. (172) the condition of $dp_{a1}/dt \to 0$ is added.

Eq. (168) corresponds to Eq. (159) for the infiltration rate, Eq. $(169)_1$ and Eq. $(169)_2$ to Eq. (160) and Eq. (97), respectively, for the moisture profile; Eq. $(170)_2$ corresponds to Eq. (89) for the advancing velocity of the wetting front, and Eq. (173) to Eq. (165) for the moisture content in the transmission zone. As θ'_* and f'_∞ can be determined by putting the denominator of the integrand in Eq. $(169)_2$

to zero, it is determined that $\theta'_* \approx \theta'_c$ and $f'_\infty \approx \{K(1-A)\}'_c \theta_c/\theta'_c$. Then both the moisture profiles agree with another. And as it can be considered that $\theta_c \approx \theta'_c$, the residual correspondences also largely agree with each other. It is known that Eq. $(172)_2$ corresponds to Eq. (105) for the change of pore-air pressure with time and Eq. (171) to Eq. (107) for the profile of pore-air pressure. As $\theta'_* \approx \theta_* = \theta'_c$ in the latter and if it can be assumed approximately in the former that $u(\tau) = u_0 = 0$ in Eq. (105), both correspondences are satisfactory.

6. Comparison of approximate solutions with experimental results[18,19]

6.1 Parameters of quasi-saturated zone

It is neccesary in the calculation of approximate solutions to find out the parameters $\alpha(t)$, $\beta(t)$, θ_1, $\hat{K}$ and ψ_e in advance. If these parameters are known, the infiltration rate, $f(t)$, can be determined by solving Eq. (149). The development of quasi-saturated zone, $x_1(t)$, is given by Eq. (140) using $f(t)$. The change of moisture profile with time is given by Eq. (148) using $f(t)$, $x_1(t)$, and the profile of pore-air pressure is determined from Eqs. (151), (115) and (116) by using $f(t)$.

The development of the quasi-saturated zone could not be known exactly due to the inaccuracy of measurement. So the movement of a constant moisture content θ'_1 which is a little smaller than θ_1 is shown in **Fig. 21.** It is seemed from this figure that the point of $\theta = \theta'_1$ approaches a finite depth asymptotically as time goes by.

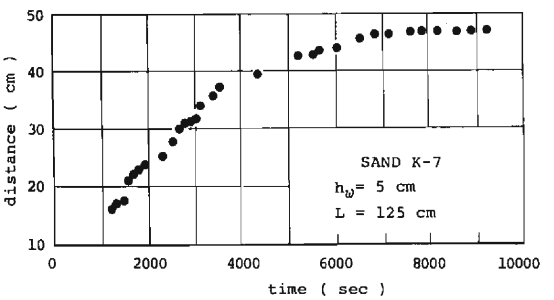

Fig. 21. Advancement of water with a high and constant moisture content, in the case of Sand K-7.

As θ'_1 is less than θ_1, the quasi-saturated zone develops in a similar manner to the point of θ'_1. This means that $x_1(t)$ does not continue to increase. So, it is known that $x_1(t)$ must satisfy the following inequality due to Eq. (14) and Eq. (159), because $\alpha_r > 0$, $\beta_r > 0$.

$$\alpha_c < \frac{\{K(1-A)\}_c}{\hat{K}} \tag{174}$$

Applying the value of hydraulic conductivity at 90% saturation to $\hat{K}$, as mentioned below, the value of the right hand side of Eq. (174) becomes about 0.67 for Sand K-7.

As, however, Eq. (174) is known to be the very weak condition for the determination of the value of α_c, it is required that the value of α_c be determined by a trial and error method as mentioned later.

Let us determine the function of $\alpha(t)$. The relations between the experimental value of $\alpha_*=(\alpha_r-\alpha_c)/(\alpha_0-\alpha_c)$ obtained by Eq. (118) and the square root of time elapsed are shown in **Fig. 22**(**a**) and (**b**), corresponding to **Fig. 18** and **Fig. 19**, respectively. In these figures, it is assumed that $\alpha_0=1$, which is the value of α_r at $t=0$, and $\alpha_c=0.28$ for Sand K-7 and 0.30 for Sand K-6, obtained later. From these figures, it is known that $\alpha_*(t)$ is given the following relation.

$$\alpha_*(t) = e^{-\lambda t^{1/2}} \tag{175}$$

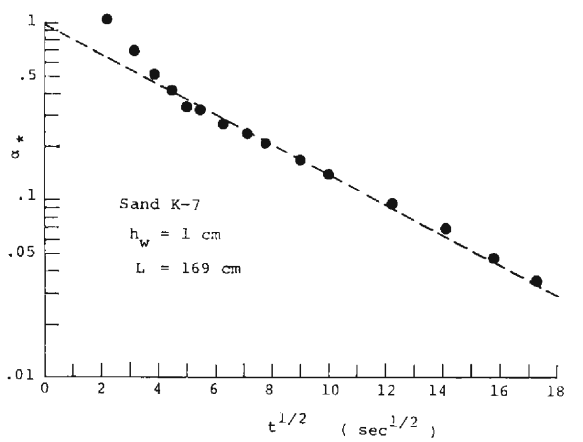

(a)

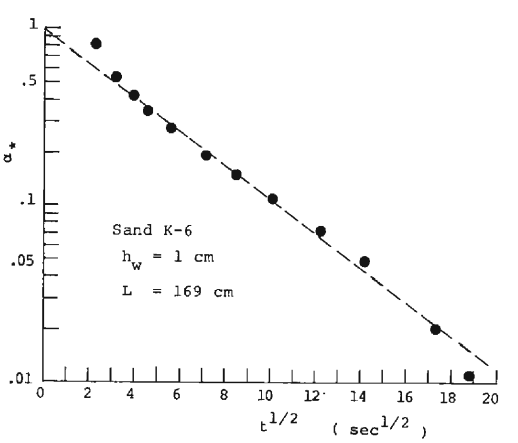

(b)

Fig. 22. Change of α_* with a square root of elapsed time.
(a) Sand K-7
(b) Sand K-6

where $\lambda=0.19$ sec$^{-1/2}$ for Sand K-7 and 0.21 sec$^{-1/2}$ for Sand K-6. Eq. (175) can be rewritten as follows:

$$\alpha_r = \alpha_c+(\alpha_0-\alpha_c)e^{-\lambda t^{1/2}} \tag{176}$$

So, considering that α is approximately equal to α_r, $\alpha(t)$ is given by Eq. (176).

Though it is known in **5.1** that $\beta_r(t)$ shows a slight tendency to decrease as time goes by, let us consider $\beta(t)$ as $\beta_r(t)$ and then approximate $\beta(t)$ to β_c given by Eq. (124).

The volumetric moisture content θ_1 just beneath the quasi-saturated zone is assumed to be equal to 90% saturation. The equivalent permeability of water in the quasi-saturated zone $\hat{K}$ is considered equal to the hydraulic conductivity at $\theta=\theta_1$.

The permeability of pore-air $K_a(\theta)$ is as follows. The function of $K_a(\theta)$ containing a unique parameter A is given by Eq. (71). As the final infiltration rate f_∞ is given by Eq. (159), adjusting the value of A, we can find out such a A value that $\{K(1-A)\}_c$ becomes nearly equal to the observed value f_∞. For example, in the case of Sand K-7, we can obtain about 3.5×10^{-3} cm/sec as the value of f_∞ by referring to **Table 2**. From this, we get about 1.8 as the value of A satisfying the relation $f_\infty=\{K(1-A)\}_c$. This means that the resistance of air movement increases with time, because the value of A is about 1 at the beginning of infiltration as mentioned in **4.1**. In the case of Sand K-6, we get $A=1.9$ by the same method.

We know that the value of ψ_e corresponds to the water or air entry value. It is meaningful to give here such a statement that, especially for the pore-air pressure at the bottom of sand layer, the observed value agrees well with the one calculated by using water entry value as ψ_e.

6.2 Comparison of observed results with calculated ones

Fig. 10(a), **(b)** and **(c)**, given in **2.2** (2), also show the comparison of the observed values with the calculated ones described by a broken line for the infiltration rate and the pore-air pressure at the bottom of layer. **Fig. 23** shows the comparison of the observed depths of the wetting front with the calculated ones described by a broken line, in which the wetting front is defined by $\theta=0.15$ and the observed values correspond to **Fig. 10**, including other experimental results. These calculations are done by using $\lambda=0.19$ sec$^{-1/2}$ and $\alpha_c=0.28$. The determination of value of α_c is carried out as follows. **Fig. 24(a)** and **(b)** show the calculated depth of wetting front and pore-air pressure at $x=L$ for Sand K-7, respectively, by using 0.24, 0.19, 0.15 sec$^{-1/2}$ as the value of λ and $\alpha_c=0.28$. From these figures, it is seen that there is no effect of λ on the depth of wetting front and that the pore-air is affected by λ only at the early stage of infiltration. Moreover, after calculating by setting $\lambda=0.19$ sec$^{-1/2}$, changing the value of α_c within $0.2\sim0.4$, it is known that the pore-air pressure is especially affected very much by α_c. Using a trial and error method, it is determined that $\lambda=0.19$ sec$^{-1/2}$ and $\alpha_c=0.28$ which is such a value of α_c that the observed pore-air pressure almost agrees with the calculated ones.

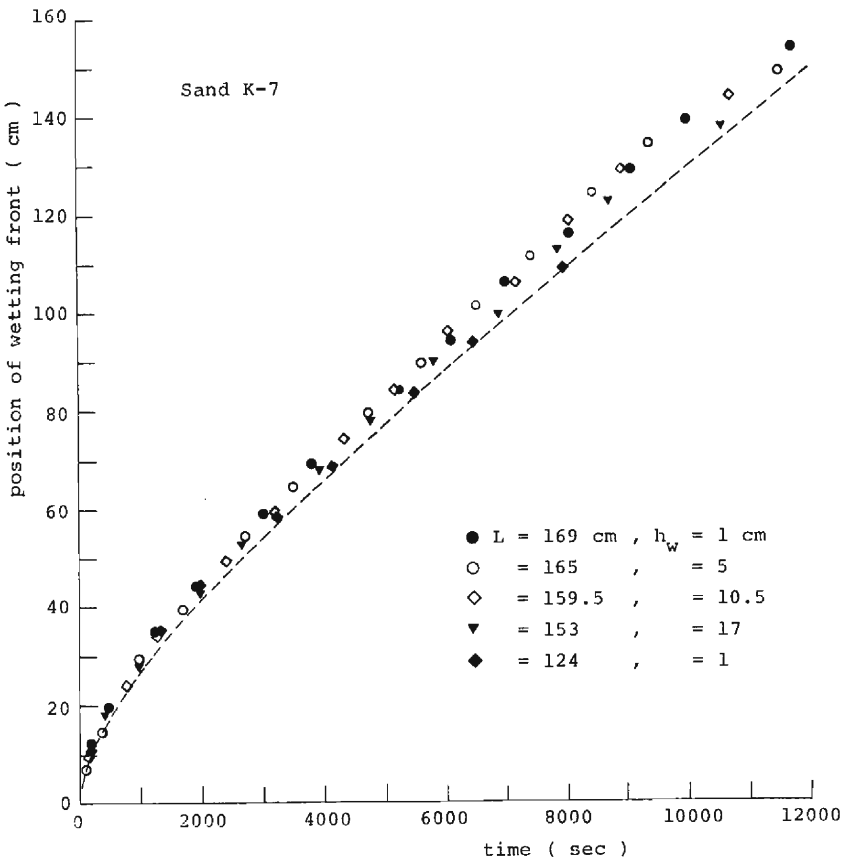

Fig. 23. Comparison between calculated depth of wetting front and observed ones, in the case of Sand K-7.

The same comparisons for Sand K-6 are shown in **Fig. 11**, already given, and **Fig. 25**. It is determined that $\lambda=0.21\ \mathrm{sec}^{-1/2}$ and $\alpha_c=0.30$.

Fig. 26 shows the development of the quasi-saturated zone calculated for Sand K-7. As the value of α_c, determined above, satisfies the condition Eq. (174), there appears the property that $x_1(t)$ approaches the critical value $x_{1\infty}$, shown by a broken line, asymptotically. $x_{1\infty}$ is given by applying Eq. (121), Eq. (122), Eq. (124) and Eq. (159) to Eq. (140) as follows:

$$x_{1\infty} = -\alpha_c \hat{K} \frac{\psi_e/(1-\alpha_c)}{\{K(1-A)\}_c - \alpha_c \hat{K}} \tag{177}$$

The value of the right hand side of the above equation becomes about 20 cm for Sand K-7 and about 17 cm for Sand K-6. In **Fig. 12** and **Fig. 13** the depth of the quasi-saturated zone after a long time has elapsed, is roughly 20 cm, which coincides with the value calculated above.

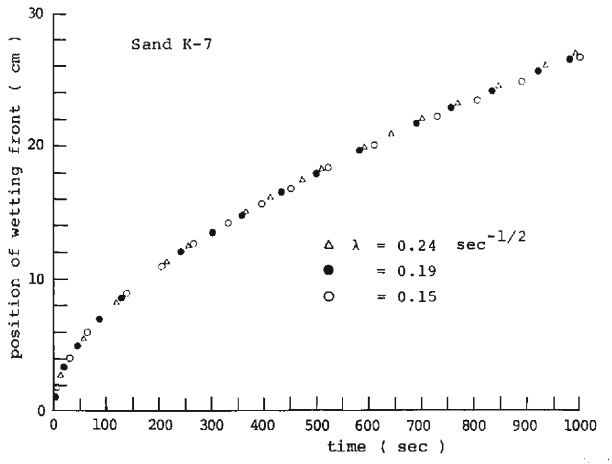

(a)

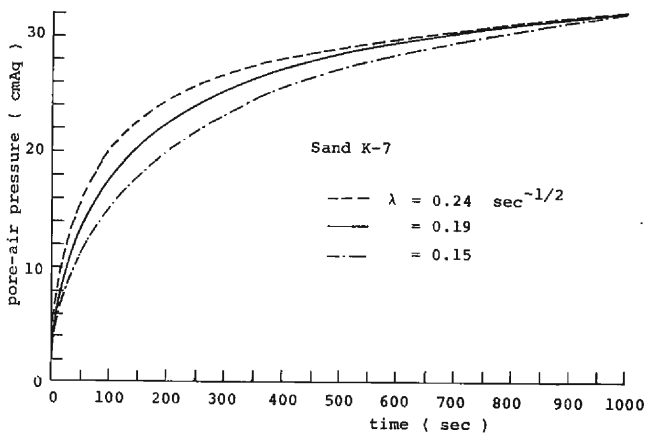

(b)

Fig. 24. Effect of λ value on calculated values, in the case of Sand K-7.
(a) Depth of wetting front
(b) Pore-air pressure at the bottom of layer

Let us examine the value of $K_a(\theta_1)$ and $\hat{K}_a$. $\hat{K}_a$ is expressed from Eq. (25) as follows:

$$\hat{K}_a = \frac{\alpha_r}{1-\alpha_r} r\hat{K} \tag{178}$$

Putting $\alpha_r \to \alpha_c$ and $r \to 1$ in the right hand side of Eq. (178), the ratio $K_a(\theta_1)/\hat{K}_a$ becomes about 3.5 for Sand K-7 and 2.9 for Sand K-6. It is known from this that the air resistance passing through the quasi-saturated zone becomes considerablely larger than that in the domain beneath the quasi-saturated zone. Though the quasi-saturated zone merely develops to a relatively shallow depth, the quasi-saturated zone

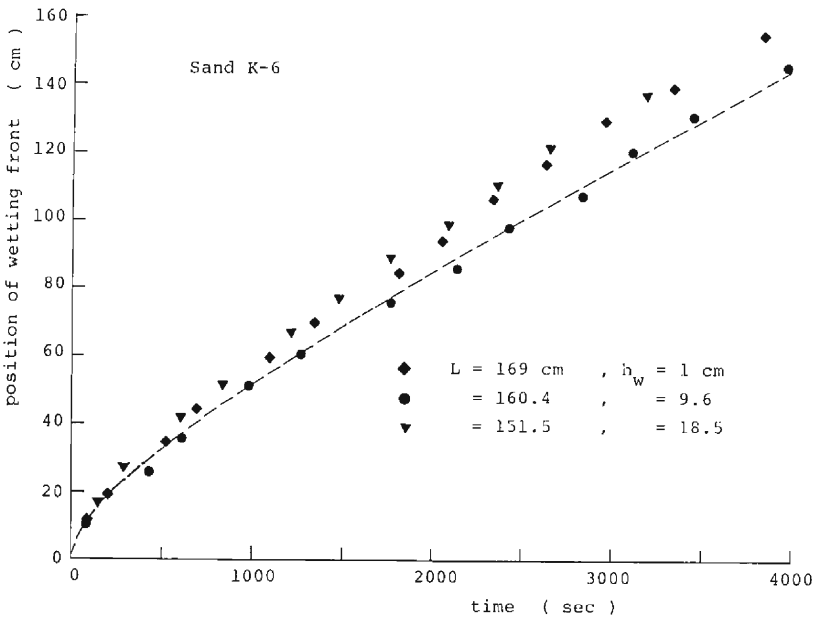

Fig. 25 Same as Fig. 23, but in the case of Sand K-6.

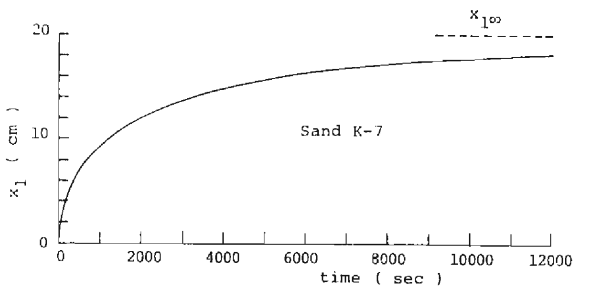

Fig. 26. Development of calculated quasi-saturated zone, in case of Sand K-7.

plays an important role in the escaping process of air. Moreover, as $1-A=K_a/(K+K_a)$ from Eq. (59), the value of $1-A$ at $\theta=\theta_1$ becomes about 0.6 in both cases of Sand K-7 and Sand K-6. As $1-A$ at $\theta=\theta_1$ is equal to α_r, in which $r\to 1$, $\hat{K}_a\to K_a(\theta_1)$ and $\hat{K}\to K(\theta_1)$ in Eq. (25), the stage where the quasi-saturated zone is being formed corresponds to such a process that the value of α decreases from about 0.6 to $\alpha_c\approx 0.3$. Therefore, this stage can be considered from a phenomenological viewpoint to be in such a process that the resistance for the air escape throughout the quasi-saturated zone is increasing.

In summary, it can be said that the results calculated by the reduced equations agree well with the observed ones for both Sand K-7 and Sand K-6.

7. Infiltration with water supply as a spray[24]

In the infiltration process with a pond on the sand column having a solid bottom, it was made clear that the existence of pore air plays an important role. In order to examine the role of pore air, an additional experiment on infiltration by water supplied through precipitation is carried out. After installing a spray apparatus above the same sand column as described in **2**, water is supplied as a spray, that is, simulating rainfall, with a variety of constant intensities.

It is found out from the results of many experiments that, when the intensity of water supply is relatively weak, ponding on the sand surface does not appear, but, when the intensity is strong, ponding begins to appear after a certain time has elapsed. As the final or minimum rate of infiltration f_∞ with ponding is given by Eq. (159), it is supposed that ponding would occur only when the intensity of simulating rainfall is stronger than f_∞.

Fig. 27 shows the experimental result, for Sand K-7, representing the relation between the intensity of water supply and the depth of the wetting front when ponding

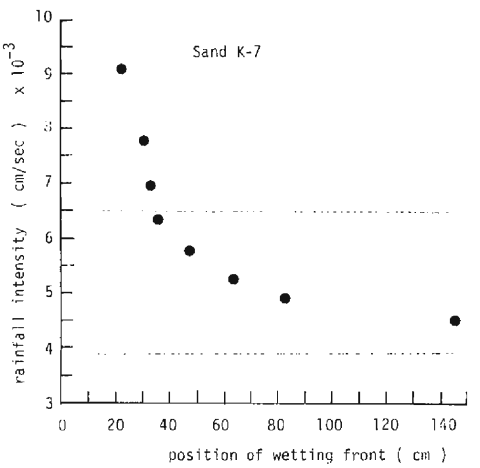

Fig. 27. Relation between the intensity of rainfall and the depth of wetting front when ponding begins to appear.

begins to appear. This is plotted by black circles. In this figure, the values of $f_\infty \approx 3.9 \times 10^{-3}$ cm/sec and $K(\theta_s) \approx 6.5 \times 10^{-3}$ cm/sec in saturation are also shown by broken lines. It is obvious from **Fig. 27** that ponding on a sand surface appears only when the intensity of water supply is stronger than f_∞ and does not appear when weaker than f_∞, as pointed out already by McWhorter[12]. As it is said that the final rate of infiltration on a sand column with screen bottom is equal to $K(\theta_s)$[25], pore air makes the penetration of water into a sand column with a solid bottom difficult. Due to this experiment, a role of pore air in the infiltration process was also disclosed.

8. Conclusion

The experiment of ponded infiltration under the condition of a constant water depth was carried out by using a homogeneous and initially air-dried sand layer with a solid lower boundary, and then the analysis of mechanism on such an infiltration was undertaken.

The results obtained are summarized as follows:

1) The moisture profile is composed of two zones. In order of depth, one is the quasi-saturated zone which develops just under the sand surface and is nearly saturated, and another is the unsaturated zone which develops just under the quasi-saturated zone. The unsaturated zone has a transitional zone from the quasi-saturated zone, the wetting front, having a relatively small moisture content, at the lower end of unsaturated zone and the transmission zone between them. As time goes by, the quasi-saturated zone declines in development and approaches a relatively shallow certain depth asymptotically. On the other hand, the unsaturated zone continues to develop accompanied by the downward movement of the wetting front.

2) Pore-air escapes from the sand surface intermittently. Although, strictly speaking, an infiltration phenomenon is discontinuous, it is possible to consider such an infiltration process as to be continuous in average. And water and pore-air in the unsaturated zone beneath the quasi-saturated zone each obey the generalized Darcy's law, and the filter velocity of water in the quasi-saturated zone and the pore-air pressure at that lower end becomes:

$$\hat{v} = \alpha_r \hat{K}\left\{1+\frac{\beta_r/\alpha_r}{x_1}\right\}$$

$$p_{a1} = (1-\alpha_r)x_1-\psi_1+p_{w0}-\beta_r\,,$$

respectively,

where $\alpha_r = \hat{K}_a/(\hat{K}_a+r\hat{K})\,,\quad \beta_r = \alpha_r(-\psi_1+p_{w0}-p_{a0})$

$$\hat{v}_a = -r\hat{v}$$

3) Just after an infiltration begins, α_r decreases abruptly from about 0.6, and approaches a constant value α_c (about 0.3 in Sand K-7 and Sand K-6) asymptotically. β_r continues to decrease, but as the degree of decrease is relatively small, β_r can be considered a constant value $\beta_c=-\alpha_c\psi_e/(1-\alpha_c)$, where ψ_e is the water entry value. And $r(t)$ is nearly equal to 1, excluding the early stage of infiltration.

4) The stage where the quasi-saturated zone is being formed corresponds to such a process that the pore-air pressure ahead of the wetting front increases and attains roughly to the value of sum of $|\psi_e|$ and the ponding depth. At this stage, the resistance for air escape throughout the quasi-saturated zone increases. At the stage where the quasi-saturated zone has developed, the resistance for air escape throughout the quasi-sasturated zone becomes at least several times (about 3 times) larger than that in the unsaturated zone beneath it.

5) The condition for escape of air in the unsaturated zone is determined at the

lower boundary of quasi-saturated zone. And the pore-air pressure at the boundary, at the stage where the quasi-saturated zone develops, is given as:

$$p_{a1} \approx (1-\alpha_c)x_1 - \psi_e + h_w$$

6) At the early stage of infiltration, that is, at the stage where the quasi-saturated zone is being formed, the following relations are valid.

infiltration rate; $f = \dfrac{S}{2} t^{-1/2}$

movement of water; $x = \varphi(\theta) t^{1/2}$

pore-air pressure at bottom of layer; $p_{aL} = a \ln t + b + h_w$

Though the values of S and a are not determined uniquely by the degree of ponding depth and by the degree of thickness of a layer, there is such a relation between S and a that the value of a decreases as the value of S increases.

7) At the stage where the quasi-saturated zone has developed enough, the infiltration rate, the rate of change of pore-air pressure at bottom of layer with time, and the shape and celerity of wetting front become unchangeable, respectively, being independent of a thickness of layer and a ponding depth. That is,

infiltration rate; $f \approx K_c(1-A_c) = f_\infty$

rate of change of pore-air pressure

at bottom of layer with time; $\dfrac{dp_{aL}}{dt} \approx A_c' \dfrac{K_c'(1-A_c')}{\theta_c'} \approx \dfrac{A_c}{\theta_c} f_\infty$

celerity of wetting front; $\omega \approx \dfrac{K_c'(1-A_c')}{\theta_c'}$

where $\theta_c \approx \theta_c'$. And the moisture content in the transmission zone within the unsaturated zone becomes about θ_c'.

At such a stage, the depth of the quasi-saturated zone becomes:

$$x_1 \approx -\alpha_c \hat{K} \frac{\psi_e/(1-\alpha_c)}{K_c(1-A_c) - \alpha_c \hat{K}}$$

8) When water is supplied as a spray, that is, like rainfall, on a sand surface, the criterion of whether or not ponding on the sand surface appears is given as follows: ponding appears only when the intensity of water supply is stronger than f_∞.

References

1) Power, W.L.: Soil water movement as affected by confined air, J. Agr. Res., 49, 1934, pp. 1125–1133.
2) Horton, R.E.: An approach toward a physical interpretation of infiltration capacity, Soil Sci. Soc. Amer. Proc., Vol. 2, 1940, pp. 399–417.
3) Free, J.R. and V.J. Palmer: Relationship of infiltration, air movement and pore size in graded silica sand, Soil Sci. Soc. Proc., Vol. 5, 1940, pp. 390–398.
4) Wilson, L.G. and J.N. Luthin: Effect of air flow ahead of the wetting front on infiltration, Soil Sci., Vol. 96, 1963, pp. 136–143.
5) Youngs. E.G. and A.J. Peck: Moisture profile development and air compression during water uptake by bounded porous bodies: 1. Theoretical introduction, Soil Sci., Vol. 98, 1964, pp. 290–294.

6) Peck, A.J.: Moisture profile development and air compression during water uptake by bounded porous bodies: 2. Horizontal column, Soil Sci., Vol. 99, 1965, pp. 327–334.
7) Peck, A.J.: Moisture profile development and air compression during water uptake by bounded porous bodies: 3. Vertical column, Soil Sci., Vol. 100, 1965, pp. 44–51.
8) Ishihara, Y., F. Takagi and Y. Baba: Experimental study on vertical infiltration of rain-water, Disast. Prev. Res. Inst., Kyoto Univ., Annuals, No. 9, 1966, pp. 551–563 (in Japanese).
9) Takagi, F. and Y. Baba: A study on mechanism of vertical infiltration, Proc. JSCE, No. 144, 1967, pp. 11–19 (in Japanese).
10) Brustkern, R.L. and H.J. Morel-Seytoux: Analysis treatment of two phase infiltration, Proc. ASCE, Vol. 96, Hy2, 1970, pp. 2535–2548.
11) Brustkern, R.L. and H.J. Morel-Seytoux: Description of water and air movement during infiltration, J. Hydrology, Vol. 24, 1975, pp. 21–35.
12) McWhorter, D.B.: Infiltration affected by flow of air, Hydrology Papers, Colorado State Univ., 1971.
13) Noblanc, A. and H.J. Morel-Seytoux: Pertabation analysis of two-phase infiltration, Proc. ASCE, Vol. 98, Hy9, 1972, pp. 1527–1541.
14) Sonu, J. and H.J. Morel-Seytoux: Water and air movement in a bounded deep homogeneous soil, J. Hydrology, Vol. 29, 1976, pp. 23–42.
15) Ishihara, Y. and E. Shimojima: Infiltration of water into confined sand column, Disast. Prev. Res. Inst., Kyoto Univ., Annuals, No. 19B, 1976, pp. 99–122 (in Japanese).
16) Ishihara, Y. and E. Shimojima: Effect of the thickness of sand layer on confined infiltration with ponding, Summary collection of lecture, Kansai Branch, JSCE, 1982 (in Japanese).
17) Philip, J.R.: The theory of infiltration: 4 Sorptivity and algebraic infiltration equations, Soil Sci., Vol. 84, 1957, pp. 257–264.
18) Ishihara, Y. and E. Shimojima: Study on mechanism of confined infiltration (2), Disast. Prev. Res. Inst., Kyoto Univ., Annuals, No. 22B–2, 1979, pp. 271–289 (in Japanese).
19) Ishihara, Y. and E. Shimojima: Study on mechanism of infiltration with ponding, Disast. Prev. Res. Inst., Kyoto Univ., Annuals, No. 25B–2, 1982, pp. 163–180 (in Japanese).
20) *e.g.* Morel-seytoux, H.J.: Introduction to flow of immiscible liquid in porous media, Flow through porous media, edited by Dewiest, R.J.M., Academic Press, 1969, pp. 483–486.
21) Ishihara, Y. and E. Shimojima: Analysis on unsaturated zone in confined infiltration, Disast. Prev. Res. Inst., Kyoto Univ., Annuals, No. 21B–2, 1978, pp. 173–191 (in Japanese).
22) Parlange, J.Y.: Theory of water movement in soil: 6. Effect of water pond over soil, Soil Sci., Vol. 113, 1972, pp. 156–161.
23) Knight, J. and J.R. Philip: On solving the unsaturated flow equation: 2, Critique of Parlange method, Soil Sci., Vol. 184, 1974, pp. 407–416.
24) Ishihara, Y. and E. Shimojima: Confined infiltration with constant intensity of rainfall, Disast. Prev. Res. Inst., Kyoto Univ., Annuals, No. 23B–2, 1980, pp. 175–191 (in Japanese).
25) Philip, J.R.: The theory of infiltration:6, Effect of water depth over soil, Soil Sci., Vol. 85, 1958, pp. 278–286.

Appendix Experiment by the U-shaped tube*)

I. Apparatus and method of the experiment

The apparatus used in these experiments is shown schematically in **Fig. I.** We use a straight and air-dried glass pipe of 125 cm in length and 0.5, 0.8, 1.0, 1.2, 1.5, 1.8 and 2.0 mm in inner diameter. The U-shaped tube is arbitrarily made of any

*) Ishihara, Y. and E. Shimojima: Study on mechanism of confined infiltration (3) —Consideration by simplified model experiment—, Disast. Prev. Res. Inst., Kyoto Univ., Annuals, No. 24B–2, 1981, pp. 171–182 (in Japanese).

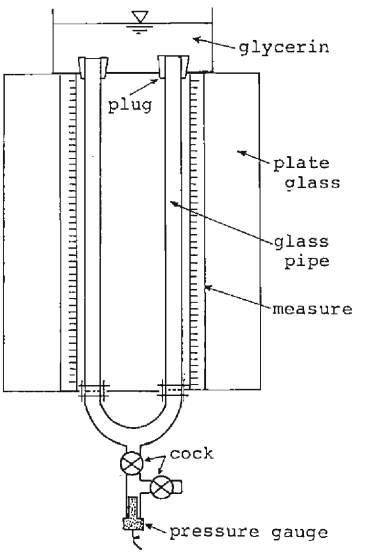

Fig. I. Schematic figure of experimental apparatus.

two pipes among them and a small U-shaped tube of 0.5 mm in inner diameter with a cylindrical bucket at the bottom. The U-shaped tube is stood vertically along the glass plate and the top part of it is inserted through the bottom of cylindrical vessel of 10 cm in inner diameter.

Glycerin is used as a penetrating fluid.

In the beginning of experiment, the fluid is poured into the vessel instantaneously as the depth of fluid to the top of the U-shaped tube becomes nearly 4 cm. As the inner diameter of the vessel is much larger than that of the U-shaped tube, the depth of fluid in the vessel remains nearly constant under experiment.

The measurement is done for air pressure at the bottom of the U-shaped tube and for the depth of the lower end of penetrating fluid. The former is measured by the very small pressure gauge which is inserted into a small bucket connected the bottom of U-shaped tube. The latter is measured by taking a photograph.

The experiment is carried out in the air-conditioning room at about 21°C for the same reason mentioned in **2.1**.

II. Results of the experiment

(a) Description of the phenonenon

The experimental result in the case of pipes of inner diameter 0.5 mm and 0.8 mm is shown in **Fig. II**, where x_f is the advancing distance of the lower end of the penetrating fluid and p the air pressure. And the detailed figure of p after the first air escape occurs is shown in **Fig. III**. In this case the air escapes from the pipe of 0.8 mm. Let us represent the inner diameter of pipe, in which the air escape occurs, as d_2, and the other as d_1. From these figures, the figures in other cases and the

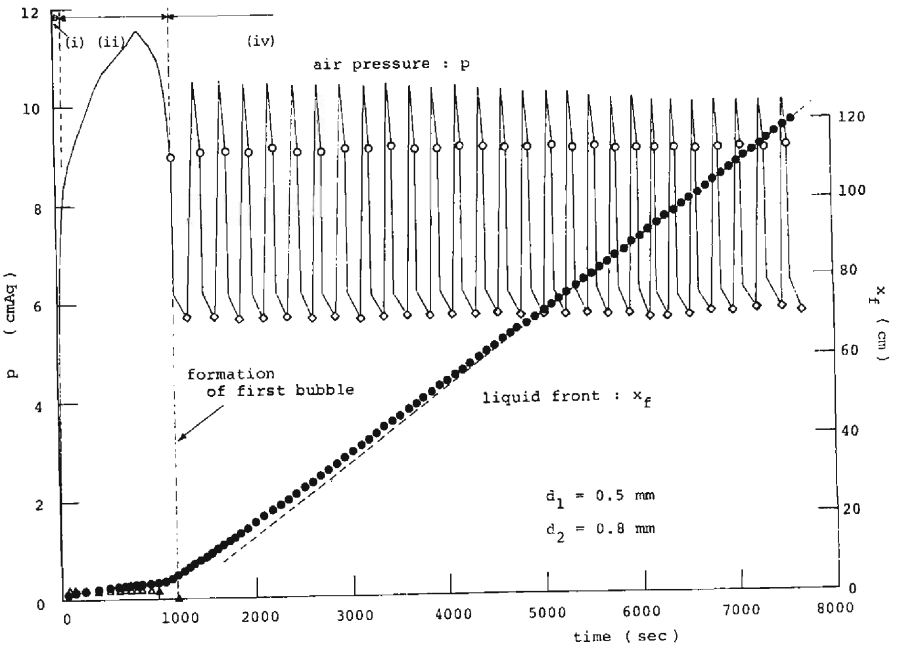

Fig. II. Changes of x_f and p with time.

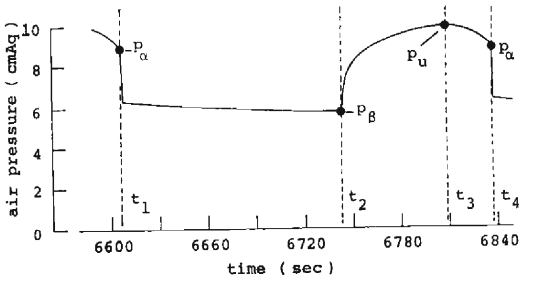

Fig. III. Detailed figure of p in the case of Fig. II.

detailed observation under experiment, the various situations under experiment are as follows, yet the statements in (i), (ii),··· showing just below, correspond to the zone (i), (ii),···, describing in **Fig. II**, respectively:

(i) The fluid begins to penetrate into both pipes as soon as the pond is formed. As a result, the air pressure increases abruptly.

(ii) The fluid in pipe d_1 continues to advance downwards with time. The fluid in pipe d_2 ceases moving downwards at a certain time and it begins to move upwards. At such a duration, the rate of increase of air pressure decreases gradually and then the air pressure begins to decrease. In some cases the up and down movement of fluid appears repeatedly in pipe d_2 for some period of time.

(iii) When the lower end of the fluid in pipe d_2 reaches the upper end of its pipe (this

corresponds to t_1 or t_4 in **Fig. III**), the air pressure begins to decrease abruptly and an air bubble begins to be formed on the upper boundary of its pipe. And then when its bubble grows to some extent (this corresponds to t_2 in **Fig. III**), it separates from the air in the U-shaped tube and, at almost same time, the air pressure begins to increase, while the fluid in pipe d_1 which is moving slowly till that time, begins to move rapidly downwards.

(iv) After that time on, the formation of air bubbles and the escape of air occur repeatedly in the same manner. However, the escape of air from the 2nd time on, occurs easily compared with the 1st time, continuing intermittently. On the contrary, the fluid in pipe d_1 advances continuously downwards in spite of the discontinuous change of air pressure.

Let us represent an air pressure when the air bubble begins to form and the air begins to escape, as p_α and p_β, respectively. p_α at the 1st time is represented by $p_{\alpha,1}$.

(b) Changes of p_α and p_β with time

After examining the results of experiments, it can be seen that the changes of p_α and p_β with time are classified into three kinds of pattern shown in **Fig. IV**(**a**), (**b**) and (**c**), where T is the period of escape of air bubble and the origin of the time axis is taken at $p=p_{\alpha,1}$. That is,

pattern (a): p_α is almost unchangeable and nearly equal to $p_{\alpha,1}$, and p_β also remains about constant,

pattern (b): p_α increases with time and then becomes more or less constant, but p_β remains constant,

pattern (c): p_α continues to increase, and p_β decreases after increasing.

If we examine the relation between the combination of both pipes and the pattern, we get **Fig. V**, where pattern (a), pattern (b) and pattern (c) are described by a black circle, a white circle and a black triangle, respectively, and the broken line satisfies the condition of $d_1=d_2$. Though the boundaries of each pattern are not clear, it is known from this figure that pattern (a) appears in case of $d_2/d_1 \gtrsim 1$, and as the value of d_2/d_1 becomes small, a change of pattern occurs, that is, pattern (a)→pattern (b)→pattern (c). Further, it can be stated meaningfully that the air does not necessarily escape from the pipe with a larger diameter of the two pipes, because there appears the case of $d_2/d_1 < 1$.

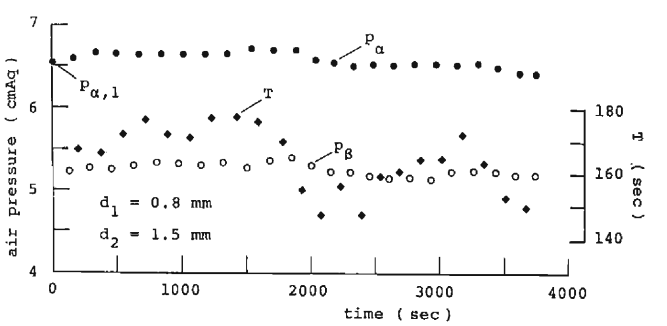

(a)

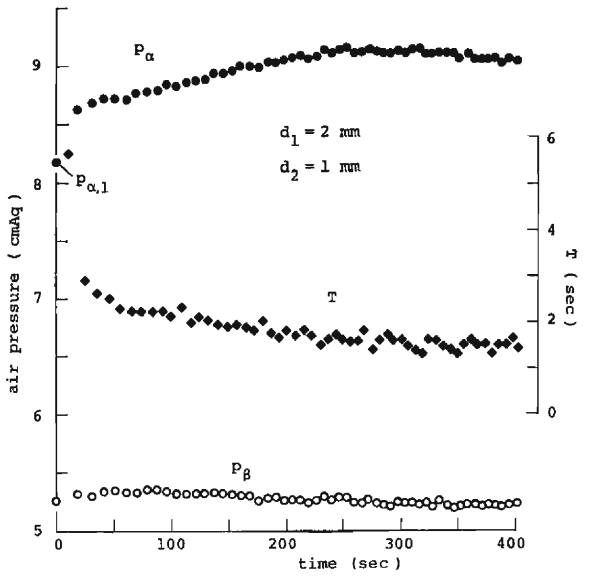

(b)

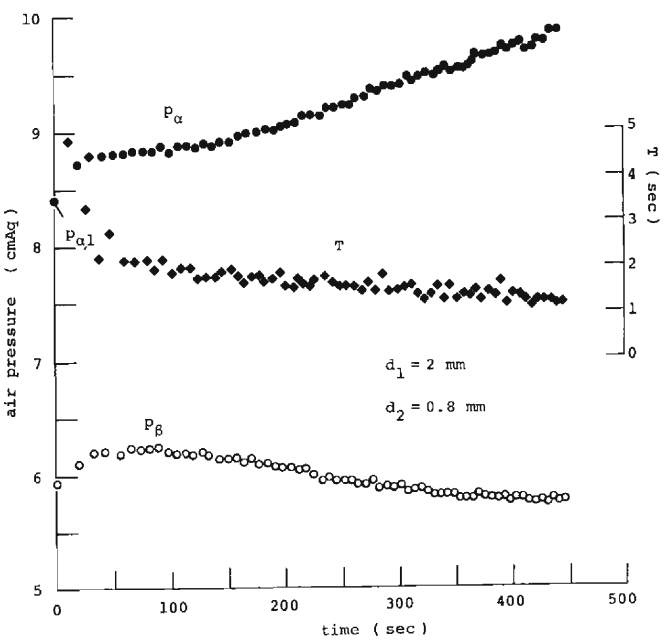

(c)

Fig. IV. Changes of p_α, p_β and T with time.
(a) d_1=0.8 mm, d_2=1.5 mm
(b) d_1=2.0 mm, d_2=1.0 mm
(c) d_1=2.0 mm, d_2=0.8 mm

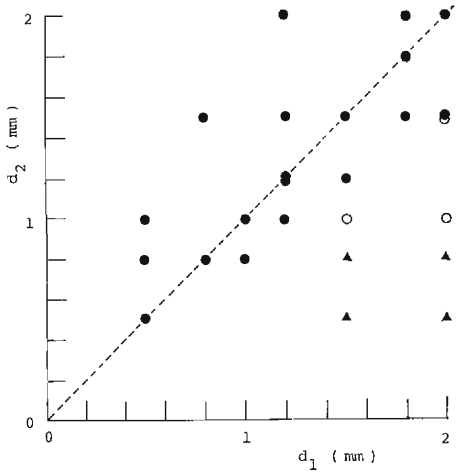

Fig. V. Regime of changes of p_α and p_β.

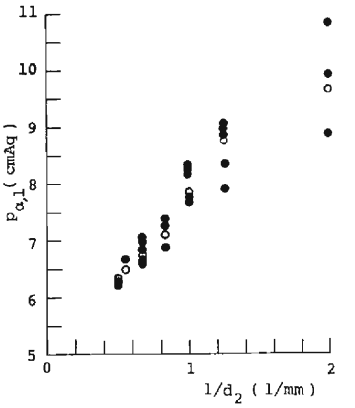

Fig. VI. Relation between $p_{\alpha,1}$ and $1/d_2$.

(c) Relation between $p_{\alpha,1}$ and d_2

The relation between $p_{\alpha,1}$ and $1/d_2$ is shown by a black circle in **Fig. VI**, where a white circle means the value p_* of sum of the ponding depth and the capillary rising height in equilibrium for the pipe d_2 estimated by other supplemental experiments. It is known from this figure that $p_{\alpha,1}$ is nearly equal to p_*, and that $p_{\alpha,1}$ is almost independent of the pipe d_1 because the black circles in each d_2 include various cases of d_1. Therefore, in the case of pattern (a) mentioned in (b), p_α is nearly equal to p_*.

(d) Relation between p_β and d_2

The relation between p_β in patterns (a) and (b), and the diameter d_2 is shown in **Fig. VII** by using a black circle and a black triangle, respectively. A white circle means the calculated value on the balance equation of force at the top of an air bubble

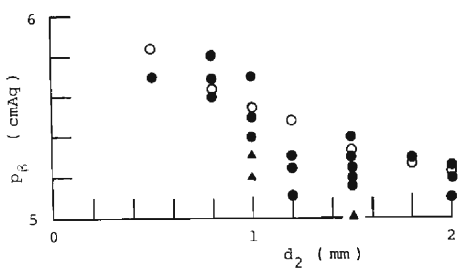

Fig. VII. Relation between p_β and d_2.

at the separation considering to be a sphere. The following two facts become claer, by this figure and the result that the size of an air bubble at the separation from the air in the U-shaped tube is larger as the value of d_2 increases. First, according as the bubble becomes large, the value of p_β decreases and becomes about 5.1 cm in water head, that is, the ponding depth. Second, the calculated value agrees approximately with the value of p_β.

III. Application of the results in the U-shaped tube to the case of infiltration into a sand column

In corresponding the phenomena in the U-shaped tube with that in the sand column mentioned in **2**, it can be considered that the formation of an air bubble in the case of a U-shaped tube corresponds to the invasion of the air in the unsaturated zone into the quasi-saturated zone in the case of the sand column, and that the separation of the air bubble from the air in the U-shaped tube corresponds to the escape of pore-air from the sand surface. Therefore, it can be expected that p_α and p_β correspond to the pore-air pressure at the lower and upper ends of the quasi-saturated zone, respectively.

(a) Condition at the lower end of the quasi-saturated zone

Pattern (c) is considered to be of such a state that the rate of penetration of fluid is larger, in average, than one of the escape of air bubbles and so the degree of compression of the air in a U-shaped tube increases with time. If we consider the stage after a long time has elapsed in the case of the sand column, we can exclude the condition as the change of p_α in pattern (c) by considering the situation of the escape of pore-air from the sand surface, explained in **2.2**(2). Therefore, we can select a constant value, either the water or air entry value, for the first approximation, as the quantity corresponding to the p_α under consideration.

(b) Condition at the upper end of the quasi-saturated zone

As mentioned in **II** (d), the observed value of p_β can be estimated approximately by calculation, and the value of p_β in patterns (a) and (b) can be approximated by the ponding depth in the case that the air escapes in large bubbles. Therefore, if we know the size of air bubble at separation, we may estimate the value of p_β.

In the case of sand column, it is difficult to determine the condition of air pressure at the sand surface by the information of the size of air bubble, because the air escapes as various sized bubbles. However, as we fortunately know the fact mentioned in **2.2**(1) that the ponding of water acts on the pore-air statically, we may use the value of the ponding depth approximately as that of pore-air pressure at the sand surface. This means that at least the condition at a sand surface may be determined approximately by the relatively large air bubbles.